Science of the Total Environment 960 (2025) 178249

Contents lists available at ScienceDirect

Science of the Total Environment

journal homepage: www.elsevier.com/locate/scitotenv

Climate-driven changes in underwater irradiance and primary productivity in an Antarctic fjord (Potter Cove, Western Antarctic Peninsula)

Dolores Deregibus[a,b,c,*], María Liliana Quartino[a], Eduardo Ruiz Barlett[d,e], Katharina Zacher[c], Inka Bartsch[c]

[a] Departamento de Biología Costera, Instituto Antártico Argentino, San Martín, Buenos Aires, Argentina
[b] Consejo Nacional de Investigaciones Científicas y Técnicas (CONICET) Buenos Aires, Argentina
[c] Alfred Wegener Institute, Helmholtz Centre for Polar and Marine Research, Bremerhaven, Germany
[d] Departamento de Oceanografía, Instituto Antártico Argentino, San Martín, Buenos Aires, Argentina
[e] Facultad de Ciencias Exactas y Naturales, Universidad de Buenos Aires, Ciudad Autónoma de Buenos Aires, Argentina

HIGHLIGHTS

- First long time series of continuous underwater irradiance measurements in Antarctica
- Increased turbidity results in decreasing underwater irradiance in Potter Cove
- Productivity of macroalgae possibly hampered during warmer years by lower light budget

GRAPHICAL ABSTRACT

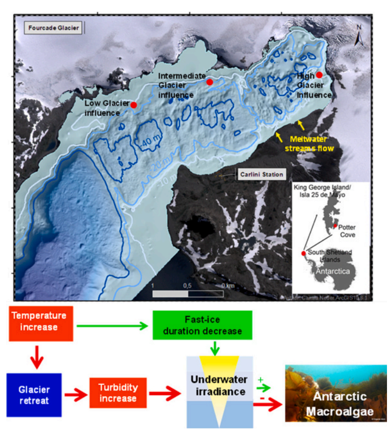

ARTICLE INFO

Editor: Christian Herrera

Keywords:
Macroalgae
Carbon balance
Climate change
Glacier retreat
Fast-ice
Time-series

ABSTRACT

The West Antarctic Peninsula (WAP) is a hotspot of climate warming, evidencing glacier retreat and a decrease in the fast-ice duration. This study provides a > 30-y time-series (1987–2022) on annual and seasonal air temperatures in Potter Cove (Isla 25 de Mayo/King George Island). It investigates the interaction between warming, glacial melt, fast-ice and the underwater conditions (light, salinity, temperature, turbidity) over a period of 10 years along the fjord axis (2010–2019), and for the first time provides a unique continuous underwater irradiance time series over 5 years (2014–2018). The effects on the annual light budget in the water column were studied along the fjord axis in three areas, a low glacier influence area (LGI), an intermediate glacier influence area (IGI), and a high glacier influence area (HGI). To determine the possible impact of light limitation on the viability of benthic primary producers, the minimum annual light requirements and the daily metabolic carbon balance of two key macroalgal Antarctic species, *Himantothallus grandifolius* and *Palmaria decipiens,* were

* Corresponding author at: Departamento de Biología Costera, Instituto Antártico Argentino, San Martín, Buenos Aires, Argentina.
E-mail address: ddu@mrecic.gov.ar (D. Deregibus).

https://doi.org/10.1016/j.scitotenv.2024.178249
Received 3 October 2024; Received in revised form 18 December 2024; Accepted 20 December 2024
Available online 4 January 2025

estimated. The mean annual, autumn, winter and spring air temperature has risen during the last three decades, but summer temperatures kept rather stable. Turbidity caused by glacial melt mostly governs the underwater light climate while fast-ice duration is currently of minor importance for the annual light budget. Glacier melting differentially affected the fjord system along its axis. The three areas showed quantitative differences in turbidity and underwater irradiance varying across seasons and years. Water clarity significantly decreased within the last few years, with key macroalgal species probably not reaching their minimum annual light requirements during warmer years. This may have considerable effects on the primary productivity of the ecosystem.

1. Introduction

The annual mean surface air temperatures over Antarctica are projected to increase by 0.5 and 3.6 °C (under different emission scenarios) by 2081–2100 (IPCC AR6 WGI Table 4.2). Regional warming will most likely continue to be one of the main factors of climate forcing in Antarctica during this century (Hendry et al., 2018; IPCC, 2021a, b). The Antarctic climate variability is also influenced by the Southern Annular Mode (SAM) and regionally by other modes, including the El Niño Southern Oscillation (ENSO: El Niño–La Niña conditions) (Chown et al., 2022). The Western Antarctic Peninsula (WAP) is highly influenced by winds and air temperature driven primarily by ENSO (Yuan, 2004; Stammerjohn et al., 2008; Ruiz Barlett et al., 2018), and the SAM (Stammerjohn et al., 2008; Schloss et al., 2012). Particularly, the northern WAP is a hotspot of climate warming with a rapid increase in air temperature and significant cryosphere loss such as severe glacial retreat and strong fast-ice decline (Turner et al., 2009; Stammerjohn et al., 2012; Cook et al., 2016; Chown et al., 2022).

In coastal zones of the WAP newly ice-free areas established as a consequence of glacier retreat (Rückamp et al., 2011), with new substrates available for benthic colonization (Quartino et al., 2013; Constable et al., 2014; Lagger et al., 2017, 2018). In parallel, glacial melt is leading to increased turbidity and decreased salinity in the water column (Klöser et al., 1996; Meredith et al., 2018). These climate-driven rapid shifts may have complex consequences on the biodiversity and productivity of the coastal ecosystems (Barnes and Souster, 2011; Barnes et al., 2024, Griffiths et al., 2024). In addition, changes in fast-ice duration have been significant in the WAP (Barnes et al., 2014). Fast-ice duration is a major structuring feature of Antarctic ecosystems, regulating light, wind exposure, water column structure and nutrient availability, as well as providing physical refuge. All these environmental changes will affect the whole food web from Antarctic microbes to whales (Constable et al., 2023; Swadling et al., 2023).

Antarctic waters are characterized by strong seasonal light changes and constant low temperatures (Zacher et al., 2009). With the fast-ice breakage in austral spring, sudden high irradiances reach the water column and the benthos (Runcie and Riddle, 2006), and high light conditions prevail until warmer temperatures induce inflow of turbid melt-water from glaciers carrying fine sediments into the sea (Drew and Hastings, 1992). In addition, phytoplankton blooms, circulation patterns and wind have a major impact on the underwater light (Schloss et al., 2012). Especially in coastal areas, climate change may significantly alter the annual light budget available for primary producers as glacial melt is exacerbated, and fast-ice duration significantly reduced (Huovinen and Gómez, 2020). The onset of thawing is extremely relevant for photosynthetic organisms, especially macroalgae, as favorable light conditions are constrained to only a few months per year when they also meet the growth active phase of macroalgae in spring (Wiencke and Amsler, 2012).

In general, changes in turbidity (and thus light penetration) are mainly evident in semi-enclosed bays, more generally in coastal areas (Klöser et al., 1993; Rodrigo et al., 2016). At this scale, the question whether rising air temperatures will cause changes in the light environment in Antarctic coastal zones and how they could affect primary producers is central to understanding the future of benthic primary production (Zacher et al., 2009). Benthic primary producers generally have low light requirements (Gómez et al., 2009), however if the annual photon dose does not meet the minimum light requirements of these species, they are not able to survive (Runcie and Riddle, 2012). Given that photosynthesis in coastal areas is the most important biological process affected by light, macroalgae, besides benthic diatoms and phytoplankton, can be considered as sentinel taxa to evaluate these changes (Deregibus et al., 2020).

Among the coastal vegetated ecosystems macroalgal habitats are one of the most productive and extensive (Runcie and Riddle, 2012; Gómez and Huovinen, 2020; Duarte et al., 2022; Pessarrodona et al., 2022). Three-dimensional macroalgae ecosystems are the key primary producers along shallow coastal zones, and form nearshore marine biodiversity hotspots along the WAP (Pellizzari et al., 2023), providing food and refuge for associated fauna (Amsler et al., 2005; Campana et al., 2018, 2020; Marina et al., 2018). Macroalgae are globally important for carbon capture and export (Krause-Jensen and Duarte, 2016; Ross et al., 2023), but also vulnerable to climate change (Hanley et al., 2023). In Antarctica, most of the carbon captured by macroalgae in newly ice-free areas, is stored as standing stock, but potentially sequestered as Blue Carbon if transported into deep areas (Quartino et al., 2020). Our study is performed in Potter Cove (Fig. 1), King George Island/Isla 25 de Mayo, located in an archipelago at the northern WAP. Recent studies especially focused on the impacts of climate-forced glacier retreat across the entire coastal ecosystem (Sahade et al., 2015). As elsewhere, benthic organisms have colonized newly ice-free areas in Potter Cove (Quartino et al., 2013; Lagger et al., 2017), and in parallel the benthos became affected by freshwater input, sediment run-off and calving of glaciers (Sahade et al., 2015; Jerosch et al., 2019).

Here, for the first time we provide a unique dataset of continuous underwater irradiance from three areas differentially affected by glacier melting along an Antarctic fjord axis for five years (2014–2018). In addition, we provide long-term data on air temperature over three decades (1987–2020). We analyzed the associated interannual, seasonal and spatial variability of the underwater irradiance, turbidity, salinity and water temperature along the fjord axis between 2010 and 2019. In addition, we provide data on fast-ice duration in the cove during the last decade (2009–2019). These data are used to generate a conceptual figure about the impact of unusually warm years on the minimal annual light requirements and on the daily metabolic carbon balance of two key macroalgal species. We hypothesized (a) that the annual and seasonal mean air temperature has been increasing in Potter Cove for the past few decades, (b) that in Potter Cove, the underwater annual light budget is stable over the years as the expected increase in turbidity, and the earlier fast-ice breakup will compensate each other, and as a consequence (c) the minimum light requirements for macroalgae are met even during warmer years. Finally, we estimate the possible consequences for benthic primary producers in Antarctic coastal zones subjected to climate change.

2. Methods

2.1. Study site

The study was carried out in Potter Cove (62° 14 'S, 58° 38' W), Isla 25 de Mayo/King George Island, South Shetland Islands, Antarctica (Fig. 1). All activities took place at the Carlini Scientific Station/

Dallmann Laboratory. Inside the cove, three areas were selected to measure environmental variables: LGI (low glacier influence area, 62° 13' 45.7" S; 58° 41' 24" W), IGI (intermediate glacier influence area, 62° 13' 33.3" S; 58° 39' 52,6" W), and HGI (high glacier influence area, 62° 13' 30,8" S; 58° 38' 29,5" W. We define "glacier influence" as impacted by sediment inflow resulting in decreased light penetration, both as a result of glacial melt.

This fjord is surrounded by the Fourcade Glacier at its eastern end and opens to Maxwell Bay (25 de Mayo Bay) to the west. It is <50 m deep in the inner cove and has some meltwater streams on the south shore, characterized by sand and gravel. In general, the surface circulation in Potter Cove is cyclonic (clockwise) related to the predominant westerly winds (Roese and Drabble, 1998). Thus, clean water enters from Maxwell Bay along the north coast (passing by IGI and LGI areas), skirts the glacier and retreats along the southern edge, being fed here by meltwater run-off (Wölfl et al., 2014). Consequently, in general the turbidity plume develops along the southern shore of the inlet and its effect is most obvious near the end of the glacier in the most inner side of the cove (HGI) (Klöser et al., 1993). Eventually, this plume may enter other areas of the cove depending on the direction and intensity of the surface wind (Hass et al., 2010; Meredith et al., 2018).

2.2. Air temperature and indicators for climate variability

Table A.1 shows an overview of environmental variables measured during the last decades in this study. Meteorological data were provided by the Argentine Servicio Meteorológico Nacional (SMN) station located at Carlini Station. Monthly averages of air temperature were calculated from daily temperatures for the period 1987–2022. From these, the annual and seasonal averages were obtained. Also, for the period 2014–2018 mean annual and monthly air temperatures were calculated for comparison with the continuous underwater irradiance dataset. We defined the seasons in the following way: summer (December 21th-March 20th), autumn (March 21th-June 20th), winter (June 21th-September 20th) and spring (September 21th-December 20th).

Climate variability indicators used in this study are the Bivariate ENSO (El Niño–Southern Oscillation) Time Series (BEST) and SAM (Southern Annular Mode) indices. The monthly averaged BEST index (Smith and Sardeshmukh, 2000) was retrieved from the National Oceanic and Atmospheric Administration Earth System Research Laboratory website (https://psl.noaa.gov/people/cathy.smith/best/). In this simple index, oceanic and atmospheric processes linked to ENSO are considered, and the different phases are indicated with a number: El Niño (= 1), La Niña (= −1), null (= 0). The monthly SAM index was obtained from the British Antarctic Survey (BAS, http://www.nerc-bas.ac.uk/icd/gjma/sam.html), and represents the difference in zonal mean sea level pressure between 40° and 65° S (Marshall, 2003). This index oscillates between negative and positive values.

2.3. Hydrographic data

Carlini Station is equipped with a photographic camera that

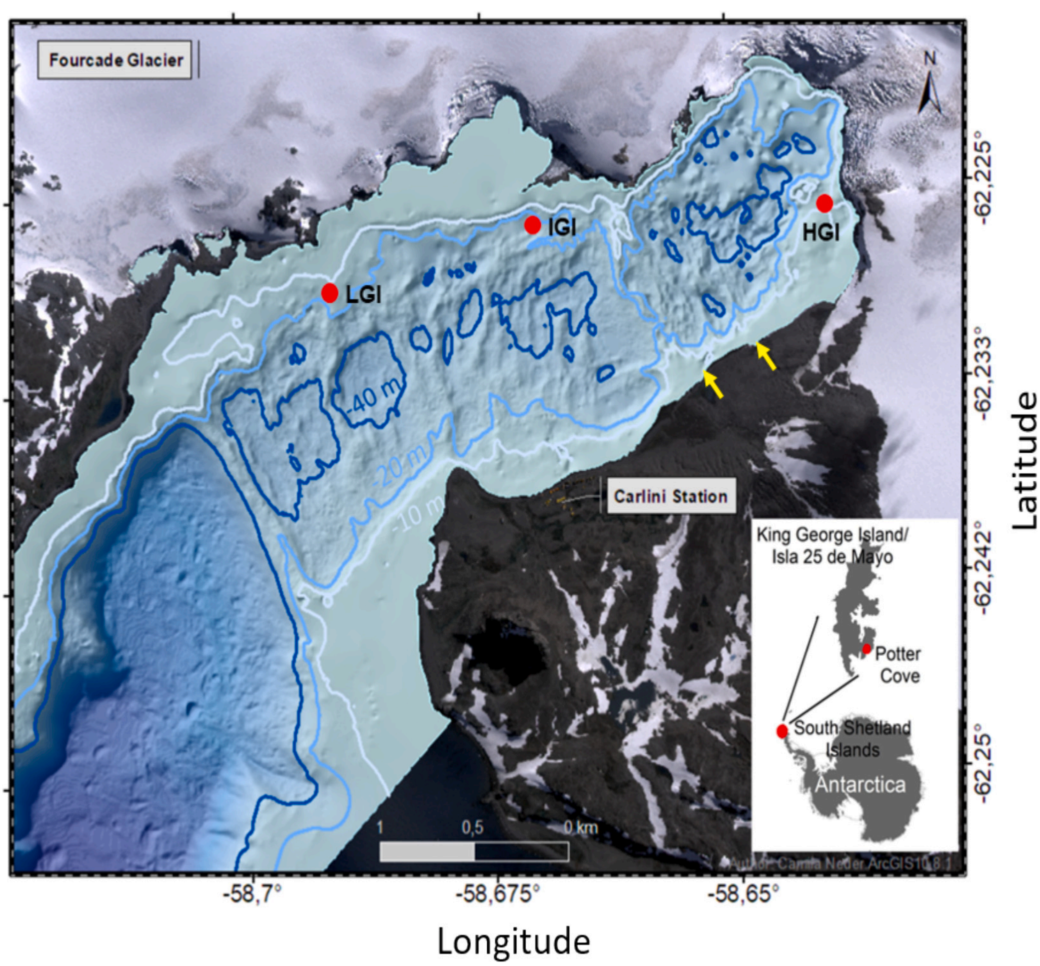

Fig. 1. The study area, Potter Cove, on Isla 25 de Mayo/King George Island (KGI). Red dots indicate sites where monitoring of abiotic variables took place: LGI (low glacier influence area), IGI (intermediate glacier influence area), and HGI (high glacier influence area). For details of variables and measurement periods see Table A.1. Lines are depth contours (map modified from Deregibus et al., 2023), and yellow arrows indicate the sites where the main meltwater streams flow into the cove.

monitors Potter Cove to determine its freezing status. This camera is located at a strategic point in order to obtain three daily images of the cove. The fast-ice duration was calculated by analyzing the daily photos of Potter Cove from 2009 to 2019 (Gómez Izquierdo et al., n.d.) and recording days and time periods with fast-ice in Potter Cove.

Photosynthetic Active Radiation (PAR) (μmol photons m^{-2} s^{-1}) was measured at 0 m (just below the water surface), 5, 10, 20 and 30 m depth using a LI-COR datalogger (LI 1400, LI-COR, Lincoln, USA) equipped with an underwater sensor LI-COR 192 PAR (LI-COR, Lincoln, USA) between 2010 and 2019. The coefficients of light attenuation (K_d) were calculated at each area using 0 and 10 m depth values according to Kirk (1994):

$$K_d = \frac{1}{z^*lnln\left(\frac{E_0}{E_z}\right)} \tag{1}$$

where E_0 is the incident irradiance at 0 m depth and E_z is the irradiance at 10 m depth. Low values of K_d indicate greater water transparency with a low attenuation of light, while high values of K_d denote the presence of high amounts of suspended particulate matter in the water column and thereby more light attenuation.

Physicochemical parameters of the water column were obtained between 2012 and 2019, using a vertical profiler SBE 19plus V2 CTD (Conductivity-Temperature-Depth), with an auxiliary sensor of turbidity ECO-NTU (Sea-Bird, USA) from pneumatic boats. The turbidity sensor measures the amount of light scattered by suspended particles in the water; the greater the scattering, the higher the turbidity. All measurements were performed at noon, and once a week (when the weather conditions were appropriate) between the surface and 30 m depth (close to the seabed) at the three sampling areas (HGI, IGI and LGI).

2.4. Measurement of continuous photosynthetic active radiation (PAR)

Continuous PAR was logged every 30 min between 2014 and 2018 at ~10 m depth in each area (LGI, IGI and HGI) with an Odyssey Photosynthetic Irradiance Recording System (Data Flow Systems, Christchurch, New Zealand), positioned upright on iron tripods and secured by SCUBA divers at the respective sites (Fig. A.1).

Every January, a new Odyssey light meter was replaced in each area. Light meters were calibrated against a LI-COR datalogger (LI 1400, LI-COR, Lincoln, USA) equipped with a LI-COR 192 PAR underwater sensor (LI-COR, Lincoln, USALICOR LI-1400) before deployment and after one year underwater (Pavlov et al., 2019). Once in the water, the light meters were checked and cleaned by divers and the data downloaded approximately once a month when conditions were favorable. The general data was corrected with the calibration factors. On some occasions, mainly at HGI, the data from the Odyssey light meters were lost due to ice disturbance or fouling. In these cases, light data was estimated. This was done by using the data obtained with Odyssey light meters from the respective neighboring area (IGI), but corrected with the instantaneous LICOR light data at the same depth (Table. A.2) from the area under consideration (HGI). Details about the stability and drift of Odyssey light meters are given in Long et al. (2012) and details about our methodology are provided in the Text A.1 of the Appendix.

2.5. Macroalgal light requirements

To determine the possible impact of light limitation on the presence of benthic primary producers in the studied areas, and during years with different mean air temperatures, the minimum annual light requirements of two abundant macroalgal Antarctic species, the endemic Antarctic brown alga *Himantothallus grandifolius* and the red alga *Palmaria decipiens* were estimated. Their light compensation point (E_c), which is the irradiance level at which the photosynthesis rate equals the respiration rate, was used to calculate the annual minimum light requirement budget (mALB) for each species by converting E_c (μmol photons m^{-2} s^{-1}) into the minimum light requirement over one year (mol photons $m^{-2}y^{-1}$) (Table 1) (Clark et al., 2013; Scherrer, 2015). As E_c values in macroalgae differ with season and depth (e.g. Franke et al., 2024), we calculated a mean E_c value per species from published evidence to harmonize the different E_c values generated from different areas, depths and seasons (Gómez et al., 2009; Clark et al., 2013; Deregibus et al., 2016).

The annual light budget recorded by light meters was calculated for an "Average year" (2014) and a "Warm year" (2016). For the definition of an average and a warm year see section 2.7. This light budget was compared to the minimum annual light budget (mALB) for *P. decipiens* and *H. grandifolius,* to detect whether these macroalgal species can reach their minimum light requirements in LGI, IGI and HGI during years with different average air temperatures. A year is considered to last from January 1st to December 31st.

2.6. Daily metabolic carbon balance

The daily metabolic carbon balance (CB) was estimated for *P. decipiens* and *H. grandifolius* using the irradiance in an "Average year" (2014) and during a "Warm year" (2016), to detect whether the CB of these macroalgal species was affected at LGI, IGI and HGI during years with different average air temperatures. The calculations of CB (mg C g^{-1} Fresh Weight (FW) d^{-1}) were performed by including (1) the average of the continuous PAR data (μmol photons m^{-2} s^{-1}) obtained at 10 m depth over the day (every 30 min) for LGI, IGI and HGI during each season, and (2) the photosynthetic parameters estimated in Antarctica from the mean values published by Gómez et al. (2009), Clark et al. (2013) and Deregibus et al. (2016) into the following P—I curve model (Jassby and Platt, 1976):

$$P = P_{max}^*tanhtanh\left(\alpha\left(\frac{average(I1:I2)}{P_{max}}\right)\right) + R \tag{2}$$

where P is the photosynthetic rate, P_{max} is the maximum photosynthetic rate, tanh is the hyperbolic tangent, α is the initial slope of the curve at low irradiance; R is the dark respiration rate, and "average (I1:I2)" is the average of two incident irradiances between time 1 and time 2 (in situ light measurements of 30 min intervals were considered). Each incident irradiance is the seasonal average of PAR measurements. The formula provides the oxygen production produced every 30 min. Hence, the sum of the photosynthetic rate values of each of the 48 intervals obtained during 24 h results is an approximation of the net oxygen production in an entire day. Calculations of daily net carbon balance (mg C g^{-1} FW d^{-1}) were obtained by converting oxygen data to equivalent carbon units using the ratio gC = 0.375 9 gO2 (Muscatine, 1980). Finally, the annual CB for each species was calculated averaging the four seasonal CB obtained for the respective year. The inclusion of in situ continuous light measurements results is a novel and more accurate approximation of the CB for each species within a specific area and/or depth (for more details see Deregibus et al., 2016).

2.7. Data analysis

To analyse anomalously warm or cold years and seasons, the anomalies of the air temperature were calculated by removing their

Table 1
Minimum annual light budget (mALB) of Antarctic macroalgae. Values were estimated from the mean compensation values (E_c) published by Gómez et al. (2009), Clark et al. (2013) and Deregibus et al. (2016), in Antarctica.

Species	mALB (mol photons m^{-2} y^{-1})
Himantothallus grandifolius	128
Palmaria decipiens	399

linear trends and the 1987–2022 climatological means (e.g. Yu et al., 2024). Then, anomalously warm or cold years or seasons were defined as periods with higher or lower mean values than the standard deviation of 1987–2022 or the respective seasonal temperature average (Schloss et al., 2012). Specifically, years and seasons were analyzed for their anomaly between 2010 and 2019.

CTD data were processed using Sea-Bird Scientific's Seasoft software package (USA) and water temperature, salinity and turbidity profiles were derived. A quality control was performed to each data set, to suppress erroneous data and salinity and turbidity outliers. Observations <0.5 m depth were removed in order to homogenize the initial value and filter surface effects in CTD sensors such as wave rugosity (Ruiz Barlett et al., 2021). Water temperature, salinity and turbidity data were averaged over the upper 10 m of the water column. Due to the very low availability of CTD profiles between January 2010 and October 2011, these data are not presented in the respective figures.

2.8. Statistics

Linear regression analyses (LRA) were performed to test whether there was a significant variation in annual and seasonal air temperature with time for the periods 1987–2022 and 2013–2022. The effect of the factor "years" was tested on the air temperature (2010–2019) with an ANOVA. The effect of the factors "area" and "years" was tested on the annual instant PAR and K_d (2010–2019), the water temperature, salinity and turbidity (2012–2019) and on the sum of the daily irradiance (2014–2018) via separate 2-way ANOVAs.

Homogeneity of variances was checked using Cochran's Test, and normality through the Shapiro-Wilks test. Post hoc multiple means comparisons were analyzed using the Di Rienzo, Guzmán and Casanoves (DGC) test. Kruskal-Wallis (KW) analyses were performed when assumptions of normality and homogeneity of variance could not be met (Di Rienzo et al., 2008).

Pearson's coefficients were calculated, annually and for summer, in linear correlation analyses between air temperature vs. water temperature, salinity, turbidity and K_d, and between turbidity vs. K_d.

All analyses were performed using InfoStat 2008 software (Di Rienzo et al., 2008). The significance level for all analyses was $p < 0.05$.

3. Results

3.1. Annual air temperature and fast-ice duration

The annual mean near-surface air temperature for Carlini Station during the period 1987–2022 and during 2013–2022 is given in Fig. 2A. It increased significantly over time, which was more pronounced during 2013–2022 (LRA, F = 6.30, p = 0.036) than over the whole period 1987–2022 (LRA, F = 4.25, p = 0.047). While the air temperature increased at an average rate of 0.25 °C per decade since 1987, the rate of increase was five times faster in 2013–2022 with 1.14 °C per decade. Specifically, the normalized and detrended air temperature series shows that during the last decade, 3 years (2016, 2021 and 2022) were anomalously warm and 2 years anomalously cold (2015 and 2019) (Fig. A.2).

Fast-ice duration in Potter Cove is given in Fig. 2B. In general, there was an inverse relationship between the mean annual air temperature and the fast-ice duration. The fast-ice duration varied from 14 to 134 days between 2009 and 2019. Since 2009, the years with the longest fast-ice duration were 2009, 2011 and 2015 (105 days y^{-1}, 134 days y^{-1}, 118 days y^{-1}, respectively) and since then the duration decreased to ≤ a month during the last two years.

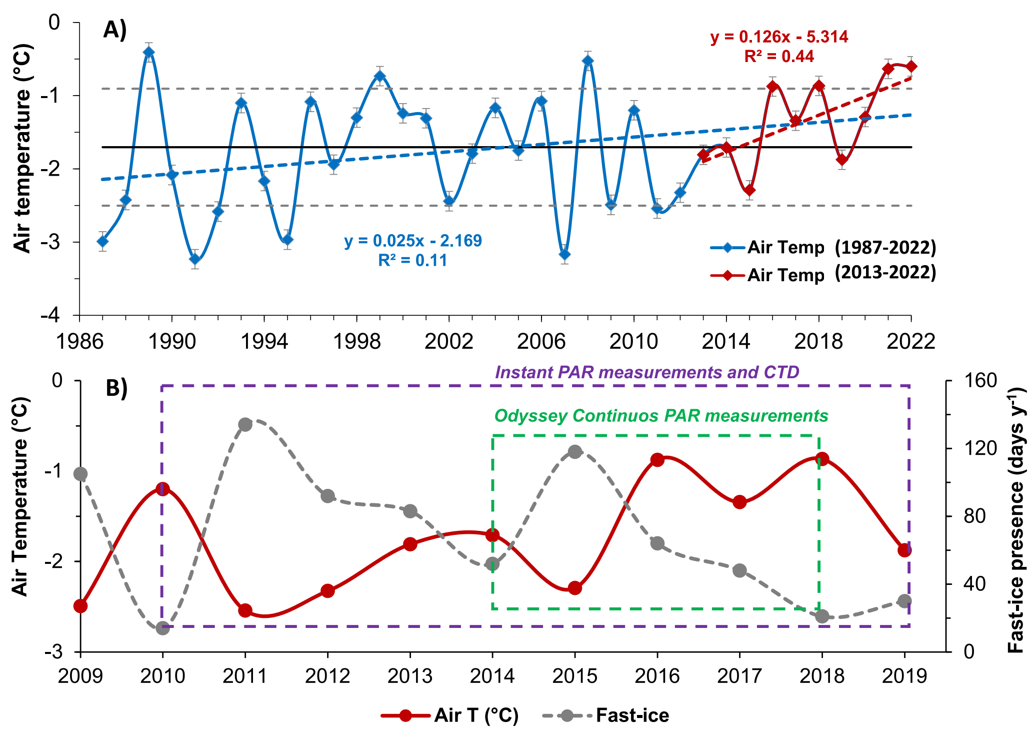

Fig. 2. A. Air Temperature. Mean annual air temperatures, overall means (blue line) and standard deviations (grey dotted lines) at Carlini station for 1987–2022. Trendlines and R^2 are given for the whole period (in black), and for the last decade 2013–2022 (in red). **B.** The purple box indicates the years when instantaneous PAR, and turbidity, salinity and water temperature were measured. The green box indicates the years when photosynthetic active radiation was measured continuously with Odyssey light meters. Data from the Servicio Meteorológico Nacional at the Carlini weather station. Fast-ice duration between 2009 and 2019 adjacent in Potter Cove, and associated measurements. Data are derived by direct observations (Gómez Izquierdo et al., n.d.; http.doi.https://doi.org/10.1594/PANGAEA.773378).

3.2. Seasonal air temperature

The seasonal evolution of air temperature in Potter Cove between 1987 and 2022 is given in Fig. 3A. Over 3.5 decades, an increase in air temperature is visible in all seasons but summer. The largest temperature increase was in autumn (0.54 °C per decade) followed by winter (0.38 °C per decade) and spring (0.01 °C per decade). But only in autumn, the mean air temperature increased significantly over time (LRA, $F = 5.36$, $p = 0.03$). The winter and autumn increase never hit the 0 °C value while this was different in spring where mean air

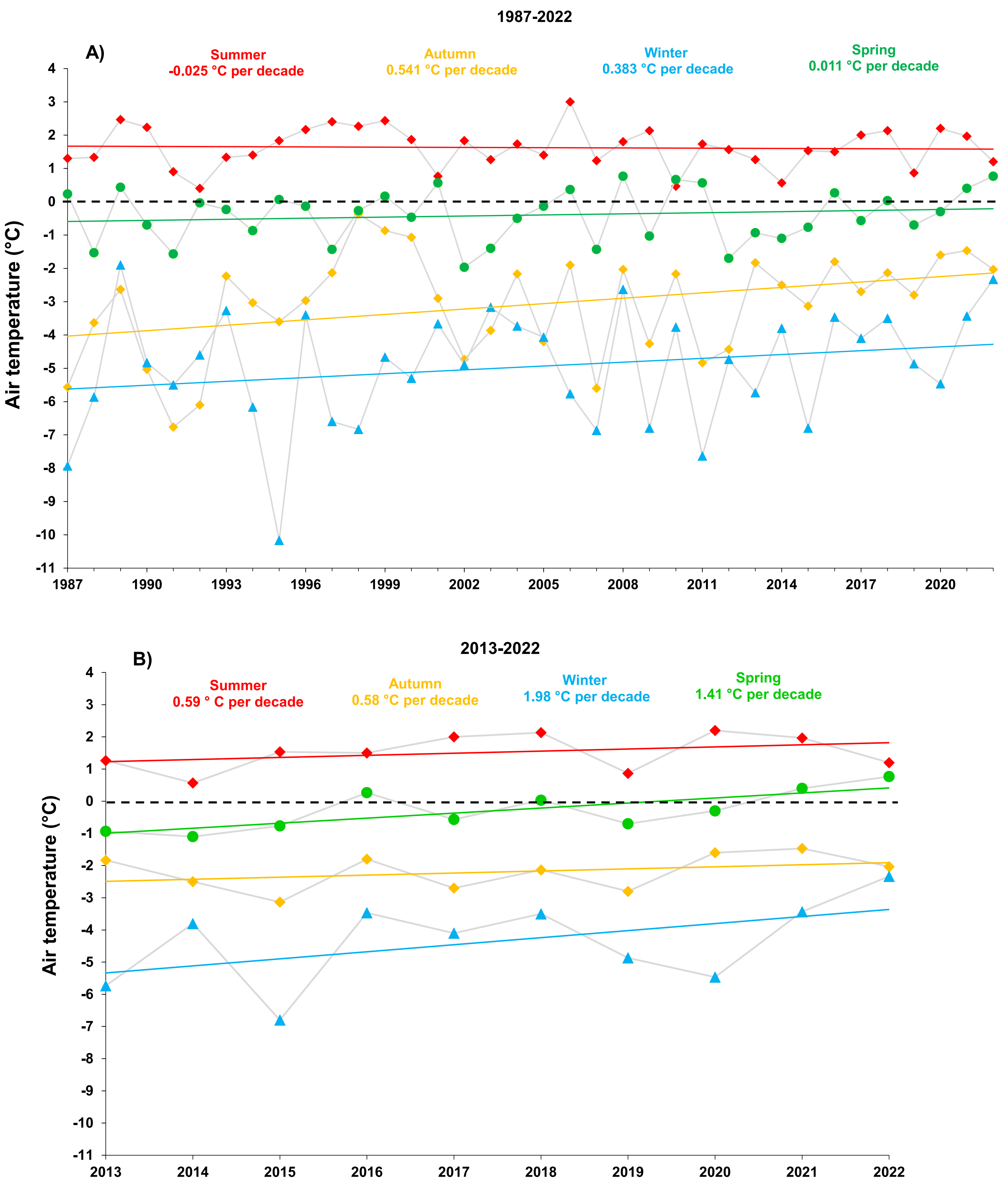

Fig. 3. Seasonal mean surface air temperature for summer (red squares), autumn (yellow squares), winter (blue triangles) and spring (green dots) at Carlini Station for the periods (**A**)1987–2022, and (**B**) 2013–2022. The colored lines are regression lines.

temperatures varied between 0.77 °C and − 1.97 °C. Considering only the last decade 2013–2022 the largest temperature increase was recorded for winter (1.98 °C per decade) followed by spring (1.41 °C per decade), summer and autumn (both with 0.59 °C per decade) (Fig. 3B).

During 2010–2019 (the time period when the instant PAR and CTD measurements were performed, and with a mean air temperature of −1.68 °C over all years), the annual mean air temperature was significantly warmer in 2010 (−1.2 °C), 2016 (−0.88 °C), 2017 (−1.34 °C), and 2018 (−0.87 °C) compared to the rest of the years (KW, H = 57.49, $p < 0.01$) (Table A.2 and Table A.3). In contrast, the years 2011 (−2.54 °C), 2015 (−2.29 °C) and 2019 (−1.88 °C) were anomalously cold (Fig. A.2).

During 2014–2018 (the time period with continuous PAR measurements) the seasonal differences in air temperature between years were not coherent. While summers were significantly different, with the summers of 2017 (1.9 °C) and 2018 (2.12 °C) significantly warmer than the summers of 2014 (0.9 °C), 2015 (1.6 °C) and 2016 (1.5 °C) (KW, H = 33.21, $p < 0.001$), the autumns 2014–2018 were similar among years. In winter, the year 2015 was significantly colder (−7 °C) than the rest of winters during this period (KW, H = 36.99, $p < 0.001$). During spring 2016 the mean air temperatures were > 0 °C (0.5 °C), and this spring was significantly warmer than all other years (KW, H = 46.94, $p < 0.001$). Furthermore, the normalized and detrended air temperature series shows that 2014 had an anomalously cold summer (0.9 °C) and spring (−1.5 °C), and 2015 had an anomalously cold winter (−7 °C) (Fig. A.3).

3.3. Water temperature, salinity, turbidity and instantaneous PAR

The temporal evolution of seawater temperature, salinity, turbidity and instant PAR across the whole water column between 0.5 and 30 m depth in each study area (HGI, IGI, LGI) of Potter Cove is given in Fig. 4 and Fig. A.4. Generally, the mean seawater temperature at HGI during the melting season was relatively cooler than at IGI and LGI (Fig. 4A). The seawater temperature was highest during the summer months with values >1.5 °C during the summers of 2015, 2017, 2018 and 2019 in all areas. Seawater temperatures >1.5 °C were also present during summer 2012 at IGI and HGI. Colder seawater temperatures (< 1.5 °C) characterized Potter Cove during summer 2014 and 2016.

Over the whole investigation period, the seawater in the superficial layer (<10 m depth) was normally less saline in summer than in the remaining months (Fig. 4B). The isohaline of 33.9 can be used as a threshold to separate the freshwater layer from more saline oceanic waters (following Meredith et al., 2018). In general, the periods with lower salinity (<33.9) in the water column were associated with warmer air temperatures. Only during the melting season of 2014 higher salinity conditions (>33.7) were present in all study areas. But, in general, surface waters nearest to the glacier (HGI and IGI) showed lower summer salinities than those in the LGI zone. However, superficial LGI seawater was also characterized by low salinities (<33.7) from 2015 onwards and thereby the area impacted by glacial melt increased (Fig. 2B). This phenomenon was associated with the observed rapid increase in air temperature measured at the Carlini Station from 2015 onwards (Fig. 2.A). As a result, this warming affected the surface layer over a larger area during the subsequent summers (Fig. 2.B). Overall, turbidity was higher at HGI, intermediate at IGI and approximately zero at LGI during the study period (Fig. 4C). During the summer months, turbidity increased up to 30 NTU in the inner cove. In a few exceptional years (2014, 2017 and 2018) high turbidity values were also observed at LGI during summer in the surface layer (<5 m depth) reaching a

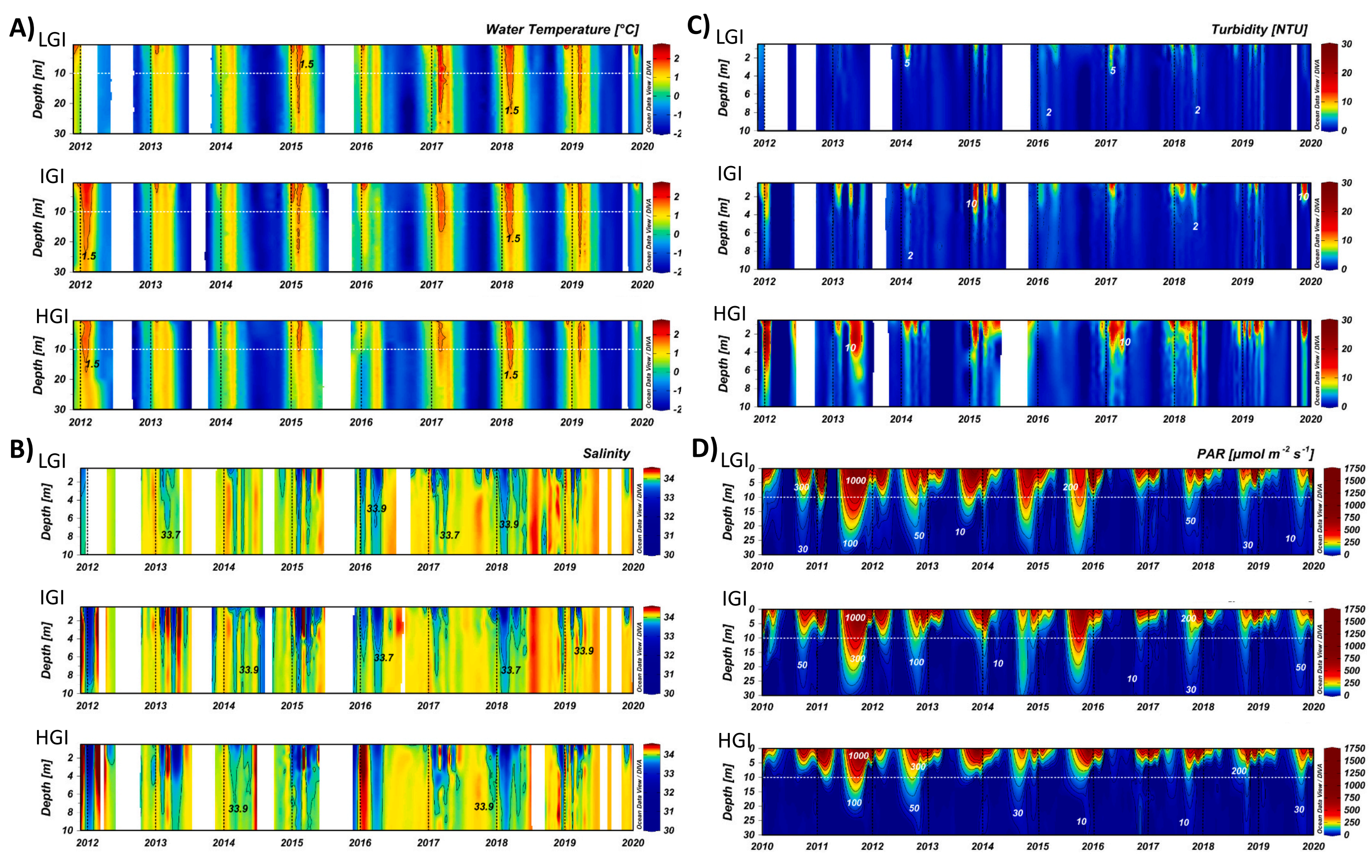

Fig. 4. Temporal evolution of water temperature (A), salinity (B), turbidity (C) and PAR (D) is depicted across three glacier influenced areas: LGI (Low Glacier Influence) in the upper panel, IGI (Intermediate Glacier Influence) in the middle panel, and HGI (High Glacier Influence) in the lower panel, between 24 November 2011 and 16 December 2019. For salinity and turbidity, the data are only given from 0.5 to 10 m depth. White areas in the panels indicate the absence of data, while black lines represent reference isolines. The dashed white line marks the 10-m isobath.

maximum of 12.6 NTU.

As expected, and in contrast to turbidity, instantaneous PAR was higher at LGI, intermediate at IGI and lower at HGI, decreasing with increasing water depth in all areas (Fig. 4D). Maximum PAR values were present in spring in all areas and during most of the studied years. However, one major result was that since 2016 a decrease in the light penetration of the water column took place during spring and summer in all three areas (in HGI mainly above 10 m depth).

The hydrographic characteristics at 10 m depth over seasons and the years 2010–2019 are visualized in Hovmöller diagrams (Fig. A.5). At this depth, in general, in each area the physicochemical parameters seawater temperature, turbidity and PAR varied seasonally. The largest changes were evident in turbidity and PAR.

The annual seawater temperature, salinity, turbidity, instantaneous PAR and K_d at 10 m depth during the time period 2010–2019 are given in Table A.2 and the respective statistics in Table A.3. At this depth, all parameters did not show an interaction between areas and years, but there was an effect of area and year for salinity and PAR, an effect of the year for water temperature, and an effect of area on turbidity and K_d. Most notably are the mean annual seawater temperature during 2014 (-0.28 °C) which was 20–50 % lower compared to the rest of the years ($p < 0.001$), and the salinity which was lower in HGI compared to LGI, and lower in 2015 compared to the rest of the years ($p < 0.001$). In addition, while at HGI the turbidity (as well as K_d) was at least twice as high compared to the rest of the areas ($p < 0.001$), the opposite was true for the instant PAR in this area with values two to three times lower

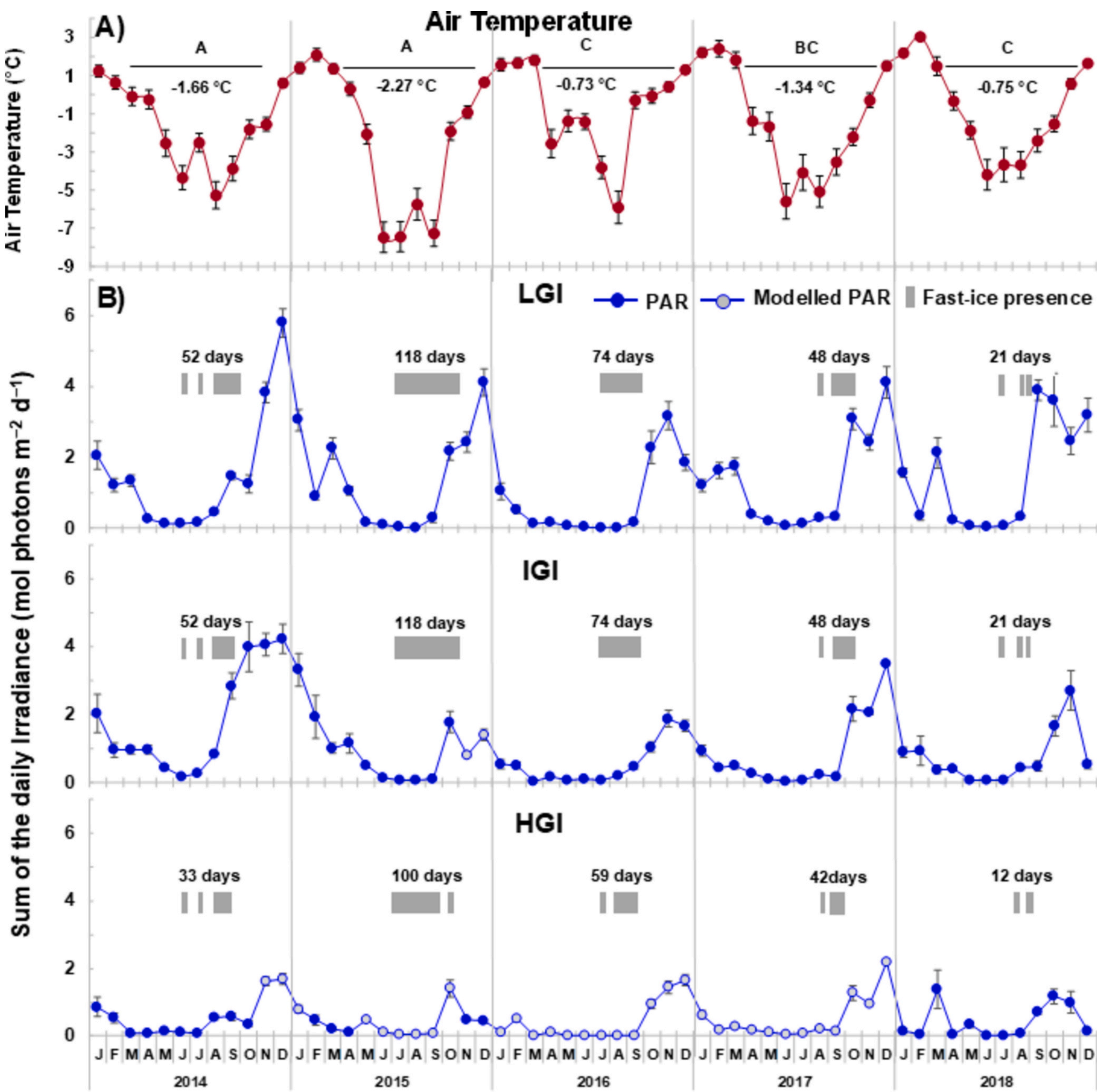

Fig. 5. Air temperature, sum of the daily irradiance, and fast-ice presence between 2014 and 2018. A) Annual mean air temperature (mean ± SE, $n = 365$); different capital letters indicate significant differences between years. B) Sum of the mean daily irradiance per month (mean ± SE) at 10 m depth; blue dots: data obtained with Odyssey light meters. Empty dots: data was estimated when Odyssey light meters were lost due to ice disturbance or fouling (Text A.1). Grey vertical bars: days with presence of fast-ice, white interfaces between grey bars indicate absence of fast-ice.

compared to IGI and LGI, respectively, and also 30 % lower at IGI compared to LGI ($p < 0.001$). Lastly, interannual differences were observed for PAR, with higher values during 2010 and 2012 compared to 2013, 2017, 2018 and 2019 ($p = 0.01$).

3.4. Correlations

In order to better show how air temperatures may influence turbidity and light attenuation, we performed linear correlations between air temperature and turbidity and K_d averaged over the surface layer at Potter Cove over the time period 2010–2019 (Table A.4, all differences $p < 0.001$). Air temperature positively correlated with turbidity and K_d in every area. Air temperature also positively correlated with seawater temperature and negatively with salinity at all locations, while K_d had a positive correlation to turbidity at all locations.

3.5. Photosynthetic active radiation: continuous measurements

The course of the sum of the daily irradiance at 10 m depth between 2014 and 2018 is given in Fig. 5. It becomes evident that PAR at 10 m depth was different among the three areas which is especially prominent from spring onwards and noticeably reduced with the onset of the austral summer. In general, the increment in the sum of the daily irradiance after the disintegration of the fast-ice was very prominent.

The annual and seasonal sum of the daily irradiance sum is given in Table 2 and the respective statistics in Table A.3. At 10 m depth, the sum for the annual, summer, autumn, winter and spring daily irradiance did not show an interaction between areas and years, but there was an effect of area and year for the annual, spring and summer irradiance, and an effect of the year in the autumn and winter irradiance.

Table 2
Photosynthetic active radiation. Sum of the mean daily irradiance over the whole year (A), for summer (B), autumn (C), winter (D) and spring (E). In brackets: standard error. Lowercase letters indicate significant differences (p<0.05) between areas per year.

A)	Annual irradiance				
Area	2014	2015	2016	2017	2018
LGI	1.69 (0.17)	1.48 (0.17)	0.79 (0.12)	1.3 (0.15)[a]	1.49 (0.21)
IGI	1.8 (0.25)	1.01 (0.18)	0.55 (0.08)	0.86 (0.07)[b]	0.71 (0.16)
HGI	0.56 (0.09)	0.39 (0.06)	0.4 (0.04)	0.52 (0.04)[b]	0.43 (0.12)

B)	Summer irradiance				
Area	2014	2015	2016	2017	2018
LGI	1.54 (0.25)	2.07 (0.62)	0.57 (0.26)	1.53 (0.16)	1.35 (0.52)
IGI	1.31 (0.35)	2.08 (0.67)	0.34 (0.15)	0.61 (0.16)	0.73 (0.17)
HGI	0.49 (0.22)	0.49 (0.17)	0.22 (0.15)	0.36 (0.13)	0.52 (0.42)

C)	Autumn irradiance				
Area	2014	2015	2016	2017	2018
LGI	0.17 (0.02)	0.44 (0.05)	0.09 (0.01)	0.22 (0.02)	0.11 (0.01)
IGI	0.51 (0.07)	0.58 (0.11)	0.1 (0.01)	0.13 (0.01)	0.17 (0.02)
HGI	0.12 (0.02)	0.24 (0.03)	0.03 (0.01)	0.1 (0.01)	0.13 (0.03)

D)	Winter irradiance				
Area	2014	2015	2016	2017	2018
LGI	0.7 (0.05)	0.11 (0.04)	0.07 (0.01)	0.25 (0.04)	1.43 (0.1)
IGI	1.31 (0.15)	0.06 (0.01)	0.24 (0.03)	0.14 (0.02)	0.31 (0.06)
HGI	0.41 (0.06)	0.06 (0.01)	0	0.14 (0.02)	0.28 (0.03)

E)	Spring irradiance				
Area	2014	2015	2016	2017	2018
LGI	3.6 (0.31)	2.9 (0.3)[a]	2.43 (0.36)	3.2 (0.32)	3.08 (0.53)[a]
IGI	4.09 (0.5)	1.32 (0.19)[b]	1.53 (0.18)	2.57 (0.16)	1.62 (0.33)[b]
HGI	1.23 (0.13)	0.78 (0.12)[b]	1.35 (0.36)	1.46 (0.09)	0.77 (0.2)[b]

Among the most remarkable results we registered that the sum of the annual daily irradiance was 2 to 3 times lower at HGI (0.46 mol photons m^{-2} d^{-1}; from now on mol photons m^{-2} d^{-1} will be abbreviated as "mpmd") compared to IGI (0.99 mpmd) and LGI (1.3 mpmd) ($p < 0.01$). Also, considering all areas together, there were interannual differences. During 2016 the irradiance was 2.5 times lower (0.58 mpmd) compared to 2014 (1.29 mpmd) ($p = 0.03$; Table 2A; Table A.5). Interestingly, only IGI showed interannual variations, with a ≥ 2 times higher irradiance during summer 2015 (2.08 mpmd) compared to the rest of the years ($p = 0.045$), and with a 2 times higher irradiance during spring 2014 (4.09 mpmd) compared to the rest of the years ($p = 0.01$, Table 2).

In summer, the irradiance was also lower at HGI (0.42 mpmd) than at IGI (1.02 mpmd) and LGI (1.42 mpmd) ($p = 0.001$), and overall, it was significantly higher during 2015 (1.55 mpmd) and 2014 (1.12 mpmd) compared to 2016 (0.38 mpmd). Also, during the summer of 2017 the irradiance at LGI was 2.5 or 4 times higher compared to IGI and HGI, respectively ($p = 0.01$, Fig. 6B). During autumn and winter interannual differences in irradiance were also present. In autumn, during 2016 (0.08 mpmd) irradiance was 3 to 4 times lower than in 2014 and 2015 ($p = 0.02$). In winter, the higher irradiance values coincided with years with a shorter duration of fast ice, and vice versa. During this season, the irradiance and in 2015 and 2016 it was much lower in comparison to 2014 and 2018 ($p < 0.01$). One major result was that in spring all areas, overall years, were significantly different to each other, with highest irradiances at LGI (3.05 mpmd), intermediate ones at IGI (2.23 mpmd) and lowest at HGI (1.12 mpmd) ($p < 0.01$). Finally, in spring also interannual differences were present, with significantly higher irradiance values in 2014 and 2017 compared to the rest of the years ($p = 0.02$, Table 2).

3.6. Macroalgal light requirements and daily metabolic carbon balance

Based on the estimated minimum annual light requirements for *P. decipiens* and *H. grandifolius* (Table 1), these macroalgae are likely to survive in two of the three study areas (LGI and IGI) during an average year like 2014. However, in a warmer year such as 2016, their survival would likely be restricted to only one of the three areas (LGI) (Fig. 6A).

In the average year the daily metabolic carbon balance (CB) was positive and higher for *H. grandifolius* (0.52–0.65 $\pm$ 0.9 mg C g^{-1} FW d^{-1}) and *P. decipiens* (2.62–2.87 $\pm$ 0.8 mg C g^{-1} FW d^{-1}) at LGI and IGI compared to negative values estimated for HGI (Fig. 6B). During the warmer year all CB values were negative for both species, except for *P. decipiens* at LGI with a CB of 0.4 $\pm$ 0.3 mg C g^{-1} FW d^{-1} (Fig. 6B).

4. Discussion

This study provides an unprecedented quantitative time series of continuous underwater irradiance measurements covering five years under differential influence of glacial melt and fast-ice duration in a coastal ecosystem located at the northern tip of the WAP. The data show a clear correlation between the air temperature and the underwater irradiance, mostly explicable by the inflow of sediments during glacial melt, and to a smaller degree to the variations in fast-ice duration. The spatial variation of the sediment surface plume in Potter Cove creates inverse gradients of underwater light and turbidity, and quantitative intra- and interannual differences in water column conditions. Over the last three decades, a significant warming of the air temperature occurred mainly in autumn and winter, while this warming trend also became prominent during spring within the last decade. In addition, water clarity significantly decreased within the last years. This possibly impacts key benthic macroalgal primary producers as we showed that two

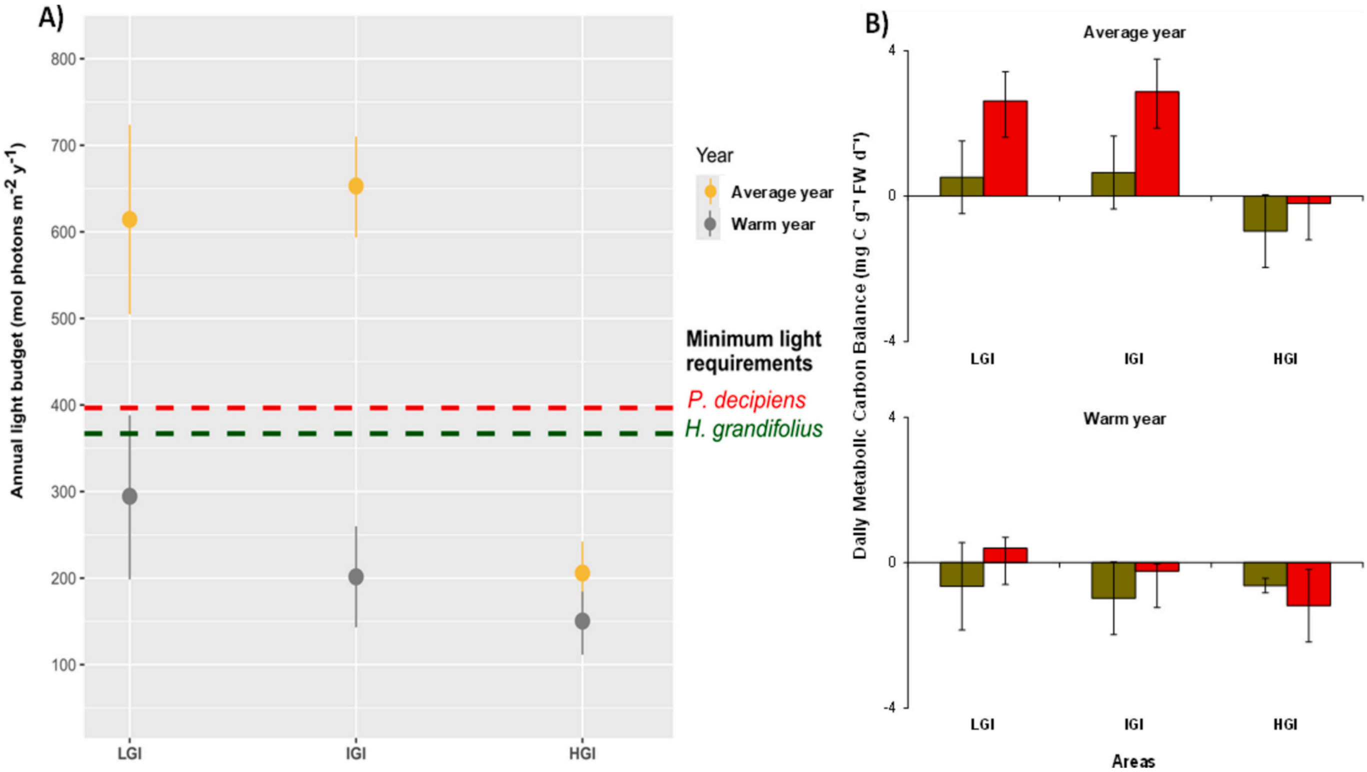

Fig. 6. **A**. Annual light budgets at the seabed. Points represent the annual light budgets recorded by Odyssey light meters during an "average year" in yellow (average year) and a "warmer year" in grey (warm year) at LGI, IGI and HGI in Potter Cove. Dashed lines are estimated minimum annual light requirements of two species of local macroalgae, *Palmaria decipiens* and *Himanthothallus grandifolius* (Gómez et al., 2009; Clark et al., 2013; Deregibus et al., 2016). Macroalgae can survive in areas where the annual light budget is above their minimum light requirements. **B**. Daily metabolic carbon balance in Antarctic macroalgae at three differently glacier influenced areas at Potter Cove. The continuous PAR 24 h data were obtained during 2014 and 2016. Values correspond to an overall net gain or loss of Carbon during 24 h.

key species may not reach their minimum annual light requirements and have negative daily metabolic carbon balances during a warmer year. The latter will probably have considerable effects on the primary productivity of this ecosystem in future considering the current climatic trends in this region. Our findings provide the baseline for productivity modelling to estimate the possible consequences for these Antarctic coastal ecosystems.

4.1. Rising air temperatures

The annual, and the autumn, winter and spring mean air temperature has been increasing, while the summer season stayed rather stable over the last 35 years. However, during the last decade (2013−2022) the air temperature increased more pronouncedly in every season compared to the long-term measurements (1987–2022). Over the last decade, the mean annual air temperature increased by 1.14 °C per decade, compared to a slower rate of 0.25 °C per decade between 1987 and 2022. If these observed trends persist, mean annual air temperatures exceeding 0 °C could be reached within 15 years (at a rate of 1.14 °C per decade) or in six decades (at 0.25 °C per decade). We observed a high number of anomalously warm years during the last decades in Potter Cove, with the last two years of our time series in a row (2021 and 2022). Considering that the occurrence and severity of extreme environmental events has been increasing with significant impacts (Siegert et al., 2023; Piñones et al., 2024), this may considerably influence primary productivity especially if occurring in spring which is the major growth season for benthic macroalgae (Wiencke and Amsler, 2012). Our findings are in agreement with the observed rapid warming of mean air temperature at the Antarctic Peninsula region since the 1950s (e.g. Vaughan et al., 2003; Chown et al., 2022; SC-CAMLR-42/BG/11, n.d.). Other studies also suggest that since the mid-2010s a more pronounced warming period has re-started (Turner et al., 2016; Carrasco et al., 2021). The IPCC Models show that in West Antarctica mean annual air temperatures may reach positive values very fast with an average air temperature of 4 °C by 2100 (IPCC WGI Interactive Atlas, n.d.). The increase in air temperature described here for 2013–2022 is also similar to a 20-year time series from the Arctic, which shows a remarkable warming in all seasons (Maturilli et al., 2015) with an annual rate of increase of 1.3 ± 0.7 °C per decade, but a maximum seasonal increase during the winter months with 3.1 ± 2.6 °C per decade.

4.2. Interaction between air temperatures and hydrography in a highly sensitive Antarctic fjord

Fast-ice is highly vulnerable to the changing climatic conditions and major decreases and interannual variations have been reported in Antarctica during the last years (IPCC AR6 WGI 9.3.2.1). In this study, at a very local scale fast-ice duration also considerably varied interannually. Since 2015, the frozen days of Potter Cove decreased drastically which is in general agreement with the situation along the WAP. Here fast-ice losses have been greatest (Stammerjohn et al., 2012) and retreated to a record low in summer 2017 (Turner et al., 2017; Parkinson and DiGirolamo, 2021). In 2022 and 2023two new records were set for the lowest annual minimum extent of fast-ice (Thompson, 2022; NSIDC, 2023; Siegert et al., 2023). Antarctic fast-ice will possibly continue to decline in future due to warming, ice sheet and ice shelf melt, and strengthening of westerly winds, although the magnitude and timing are uncertain (Swadling et al., 2023), and there are limited observations and a disagreement among models (Chown et al., 2022).

In Potter Cove there are inverse gradients of underwater light or salinity with turbidity increasing with distance from the Fourcade Glacier run-off (east end of the cove). Particularly the HGI as the area in Potter Cove most frequently and extremely influenced by glaciers, showed high turbidity and low salinity values across the entire profile of the water column. This is in agreement with previous studies in this area pointing to the sediment load and resulting turbidity as key factor determining the hydrographic characteristics in areas close to glacial outflows (Schloss et al., 2012; Ruiz Barlett et al., 2021; Braeckman et al., 2021; Neder et al., 2022). High turbidity in surface waters often associated with low salinity during the melting season has also been observed in several others Antarctic fjords in the WAP region (e.g., Lee et al., 2015; Rodrigo et al., 2016; Lima et al., 2019; Wójcik et al., 2019).

One major outcome of our study is the clear correlation of air temperatures to direct responses in the surface water layer, and to fast-ice duration. The longest fast-ice period (> 4 months) occurred during the anomalously cold winter of 2011. Similar results were obtained in Potter Cove for 2009–2017 (Ruiz Barlett et al., 2021). Very high underwater instant irradiances were recorded during the anomalously cold spring 2012 and a combination of high salinity and very high PAR values were also present during the anomalously cold summer 2014. In contrast, extremely low instant irradiances occurred during the anomalously warm year 2016. The latter coincides with the exceptional high glacier discharge rates which were about 4.5 times higher than the previous years during the warm summer 2016–2017 (Braeckman et al., 2021). A similar situation was observed with high turbidity and very low instant irradiances during the warm year 2018. We thus can confirm that glacial discharge levels are strongly dependent on local air temperature and released suspended particulate matter accumulates in surface layers generating elevated turbidity.

The two main modes of climate variability influencing the Antarctic Peninsula, the SAM and the ENSO, could have probably influenced the atmospheric conditions, and thus the nature of the cryosphere loss and of the hydrographic conditions observed in Potter Cove (Table A.6 and A.7). A good example is 2010 when El Niño coincided with a negative SAM index during the first months of the year, which turned into opposite phases during the second half of the year. This situation led to relatively colder conditions in summer, and warmer conditions in winter and spring, respectively. The summer 2010 was anomalously cold in the northernmost Antarctic Peninsula (Costa and Agosta, 2012), also with colder, more saline and low turbid waters in Potter Cove (Ruiz Barlett et al., 2021). In winter 2010 the fast-ice period was remarkably short lasting only 14 days, and breakage of fast-ice around mid-September was probably associated with warm conditions in winter and spring. This situation also influenced the annual light budget and led to significantly higher underwater PAR values during this year. The trends and relationship of parameters analyzed in this study are in agreement with previous studies (Schloss et al., 2012; Braeckman et al., 2021; Ruiz Barlett et al., 2021). All highlight that the combined effects of ENSO and SAM conditions affecting winds, air temperature and fast-ice duration act as an additional, indirect forcing factor on the environmental parameters and on the marine ecosystem of the Potter Cove.

4.3. Changes in the cryosphere influence the underwater light climate in Potter Cove?

In coves and bays such as Potter Cove, located in the WAP and especially in the South Shetland Islands, the climate is milder and the impact of rising air temperatures are very high (Ducklow et al., 2013; Chown et al., 2022). These fjords have probably the highest sedimentation rates across the Antarctic continent (Meredith et al., 2018), and hence govern the underwater light climate much more than fast-ice. Our results show the severe impact of the melting of the glacier Fourcade during summer, generating highest peaks in turbidity and thereby reducing irradiance values by >50 % compared to spring (Table 2, Figs. 4 and 5). In addition, there is a clear spatial gradient in Potter Cove creating considerable differences in the available underwater irradiance along the fjord axis. Areas with low glacier influence (LGI) have an annual daily irradiance ~30 % or > 300 % higher than areas with intermediate (IGI) and high glacier influence (HGI), respectively. Thus, the location inside a cove or bay is very important in determining the total light budget for primary producers, as the distance to the glacier (and hence the presence of particulate suspended matter), the water circulation, and the fast-ice duration greatly influence the irradiance in the water column and reaching the sea bed (Clark et al., 2013; Deregibus et al., 2016; Clark et al., 2017; Gómez and Pirjo, 2020; Niedzwiedz and Bischof, 2023; Schlegel et al., 2024). The underwater annual light budget values of 146 to 647 mol photons m^{-2} yr^{-1} calculated in this study are within the order of magnitude to those reported in other fjord systems in Antarctica (Gómez et al., 1997; Gómez et al., 2009; Clark et al., 2017), and also in the Arctic (Bartsch et al., 2016). In summer, the lowest irradiance was recorded at HGI, and during this season it was very much affected by air temperature. During the very warm summer of 2017 very low underwater irradiances were recorded in most of the cove. This probably was due to the expansion of the sediment plume and its load. Interestingly, irradiance differed significantly in spring in all three areas, unlike in summer. This pattern is consistent with the fact that average air temperatures are lower in spring than in summer, so the sediment plume contains a lower sediment load and forms a distinct turbidity gradient (Deregibus et al., 2023), which affects each area differently.

We hypothesized that in Potter Cove the underwater annual light budget is stable over the years as we assumed that an expected increase in turbidity will be compensated by the earlier fast-ice breakup. Our data indicate otherwise. In 2016, the annual air temperature was significantly warmer than in 2014, while the annual daily irradiance was significantly lower. Despite the overall warming trend, air temperature increases were not uniform across seasons. Each year exhibited distinct combinations of “cold” and “warm” seasons. In 2016, the longer fast-ice duration extended into spring, reducing underwater irradiance. This, combined with a significantly warm spring that intensified turbidity in the water column, resulted in a lower annual light budget. In contrast, 2014 featured a significantly colder summer, which improved water clarity. The latter, together with a minimal fast-ice presence during winter which enhanced underwater light availability earlier in spring, lead to a significantly higher annual light budget for this year. The year 2015 was anomalously cold, with a significantly colder summer too, favoring clear waters. This resulted in a significantly higher underwater irradiance during the first half of the year, but the overall annual light budget was only intermediate, as the high summer and autumn irradiances were followed by a 4-month long fast-ice duration lasting much longer into spring than in other years (Table 2, Fig. 5B). In summary, our data indicate that the increase in underwater irradiance following the disintegration of fast-ice was generally very abrupt (Fig. 5B). While the duration of fast-ice primarily determined the total irradiance budget during winter and early spring (Table 2), its impact on the annual light budget was less significant. Instead, the primary factor influencing both the seasonal and annual light budgets was the turbidity of the water column.

Our findings indicate that areas with an intermediate glacier influence such as the study site IGI are more prone to interannual variations of the underwater light budget, especially in spring and summer, than low and high sediment impacted areas (LGI, HGI). Areas far away from the glacier run-off as LGI, are rather independent of fast-ice variations, and the influence of the sediment plume is low. Thus, the underwater light availability is moderately high and constant over most relevant months. The opposite is true for areas close to the glacier run-off such as HGI as they are highly influenced by sedimentation during most parts of the year except for winter (Deregibus et al., 2020; Neder et al., 2020) resulting in generally low underwater light conditions. As a conclusion, areas located in the middle part of glacier influenced coves or fjord systems are likely most sensitive to subtle differences in sedimentation since they are located in the limit where the extent of the sediment plume varies the most (Jerosch et al., 2019; Neder et al., 2022). They exhibit the largest interannual variability in light conditions, and thereby they are most prone to changes in their benthic assemblage structure (Deregibus, 2017).

Although the underwater light climate was mostly explicable by air temperature conditions, some results suggest additional influencing factors. The interannual atmospheric climate variability modes which influence wind direction, cloudiness and rain, may possibly also affect the light budget. For example, during spring 2015 and autumn 2016 we registered some unexpected low irradiance values. During this period El Niño was present, which is characterized by cold air temperatures and an increased frequency of anomalous easterly winds (Yuan, 2004). However, the parallel occurrence of a positive phase of the SAM between November 2015 and March 2016 (Table A.5) was most probably responsible for reducing the effects of El Niño in this region by bringing warm and humid air and increased rainfall (e.g., Marshall et al., 2006). This found its expression in summer 2016 which was characterized by warm air and high rainfall (Ruiz Barlett et al., 2021). Both factors may have decreased the underwater irradiance.

Summing up, in Potter Cove the underwater light climate is mainly influenced by the air temperature. The year 2016 as an example of a "warm" year generates a possible scenario for the development of the underwater light budget with rising temperatures in future. During this unusually warm year the annual daily irradiance values were ~ 50 % or 200 % lower than during years with intermediate or low air temperature values, respectively, pointing to a darkening future Antarctic coastal ecosystem as is already an ongoing phenomenon in parts of the Arctic (Konik et al., 2021).

4.4. Biological perspectives towards primary productivity

The minimum light requirements (mALB) for *H. grandifolius* and *P. decipiens* calculated for 10 m depth were met with a positive carbon balance at LGI and IGI, but not at HGI during the average year. This meets our expectation as the vertical distribution limit of these species was at 30, 20 and 10 m depth at LGI, IGI and HGI, respectively during surveys in 2010 and 2013 (Deregibus et al., 2016; Deregibus, 2017). In contrast, in the warm year 2016 the modelled mALB was not achieved for both macroalgal species, at HGI and IGI and only by *H. grandifolius* at LGI. In addition, during this warm year the CB was negative for these species at 10 m depth. These results are alarming, as rising air temperatures and continuous high melting rates of the glacier Fourcade are envisaged. The annual mean surface air temperatures over Antarctica are projected to warm between 0.5 and 3.6 °C (under different emissions scenarios) by 2081–2100 (IPCC AR6 WGI Table 4.2). As a result, strong impacts on marine life in general are expected (Chown et al., 2022). The envisaged warming along the northern part of the WAP accompanied by high glacier melting rates and a lengthening of the thawing season, raises the question, whether macroalgae can store enough carbon during the shortening time periods when the minimum light requirements are surpassed to support their energy requirements for the rest of the year? If the annual photon doses do not sustain growth and reproduction of macroalgae, they will probably disappear from certain areas and depths in the short term (Runcie and Riddle, 2012). This will result in shifts in their vertical distribution to shallower depths, increasing overlap and competition between species and possibly resulting in altered community compositions and demographic patterns (Quartino et al., 2020) as has been observed in the Arctic (Düsedau et al., 2024).

In the long term, we predict that sedimentation rates will significantly decrease once the glacier has retreated enough, leading to an increase in the underwater annual light budget again. In addition, the projected decrease in fast-ice in the south of the WAP, will also support macroalgal biomass (Amsler et al., 2023). Macroalgal expansion in coastal areas is expected to reduce overall benthic biodiversity if they replace biodiversity rich faunal communities (Worm et al., 2006; Clark et al., 2013), however the primary productivity and carbon-sequestration potential of ecosystems will increase. Primary producers in general have been reported to be affected by climate change-induced glacial melt and the corresponding decline in irradiance, as was also shown for phytoplankton (Schloss et al., 2012), and benthic microalgae (Campana et al., 2020; Braeckman et al., 2021) besides macroalgae (Deregibus et al., 2016). But benthic diatoms may also thrive in close proximity to a retreating glacier (Ahn et al., 2016; Pers orbs), indicating that sedimentation may not be always detrimental to diatoms. As warming, reduced fast-ice cover and duration, and glacial melting with all associated factors such as change of ice scour, turbidity and freshening will cause regional benthic biomass variations (Griffiths et al., 2024), regular long-term studies are needed to better elucidate the possible fate of these ecosystems.

5. Conclusion

There is an urgent need to conserve Antarctic ecosystems due to their unique and high biodiversity and high endemism. Our results indicate that the effects of climate change stress and negatively impact coastal macroalgae ecosystems along the Antarctic Peninsula. In addition, the WAP is also threatened by introduction of non-indigenous species and increased tourism (Convey and Peck, 2019; Tejedo et al., 2022). Science has a major role in providing evidence-based data for policy decision makers, and for mitigating the consequences of anthropogenic climate change (Chown et al., 2022). This underscores the importance of protecting the ecosystems of the Antarctic Peninsula, reinforcing the importance of adopting the proposal of the Marine Protected Area in the so-called Domain 1 (D1MPA) (CCAMLR-43/37, n.d.), led by Argentina and Chile, which includes the Western Antarctic Peninsula and regions South of the Scotia Arc.

Macroalgae growing in Polar fjords which are heavily affected by climate change are in a constant tradeoff between being negatively affected by glacier melting and expanding into newly ice-free areas (Deregibus et al., 2020; Düsedau et al., 2024; Neder et al., 2024). In recent years, hundreds of fjords have emerged as glaciers retreated along the Western Antarctic Peninsula (WAP), resulting in significant carbon gains driven by benthic colonizing organisms (Barnes et al., 2020; Deregibus et al., 2023). Benthic blue carbon around Antarctica has the potential to mitigate broader CO_2 emissions, as it continues to increase with climate change (Bax et al., 2021; Morley et al., 2022; Ross et al., 2023; Sands et al., 2023; Tait et al., 2024). However, if the impacts of climate change intensify, macroalgal colonization in newly exposed inshore areas may only establish persistent and mature communities after the cessation of severe glacial melt (Campana et al., 2020; Deregibus et al., 2020). Until then, the potential of these inshore zones-and entire fjord systems- to support 'new or additional blue carbon' could be possibly threatened The study of Antarctic shallow ecosystems should remain a high research priority, and given the envisaged massive ecological changes, the expansion of international research cooperation is essential for the regional understanding of climate-induced impacts, for scientific progress in identifying forthcoming changes and 'tipping points' (Clark et al., 2013; Bennett et al., 2015; Deregibus et al., 2017; Barnes et al., 2021; Griffiths et al., 2024). Monitoring programs could be implemented at a regional scale (e.g. in the framework of the Southern Ocean Observing System, The Antarctic Near-shore and Terrestrial Observing System (ANTOS)) along the WAP to predict possible changes in primary productivity in areas affected by climate change, and quantify their expansion, productivity and contribution to blue carbon.

CRediT authorship contribution statement

Dolores Deregibus: Writing – review & editing, Writing – original draft, Supervision, Project administration, Methodology, Investigation, Funding acquisition, Formal analysis, Conceptualization. **María Liliana Quartino:** Writing – review & editing, Supervision, Project administration, Funding acquisition, Conceptualization. **Eduardo Ruiz Barlett:**

Writing – review & editing, Writing – original draft, Methodology, Formal analysis, Conceptualization. **Katharina Zacher:** Supervision, Methodology, Investigation, Conceptualization. **Inka Bartsch:** Writing – review & editing, Supervision, Project administration, Methodology, Investigation, Funding acquisition, Conceptualization.

Declaration of competing interest

The authors declare that they have no known competing financial interests or personal relationships that could have appeared to influence the work reported in this paper.

Acknowledgments

This work was performed at Carlini Station within the framework of the scientific collaboration between Instituto Antártico Argentino/ Dirección Nacional del Antártico and the Alfred Wegener Institute, Helmholtz Centre for Polar and Marine Research. This study was supported by the Consejo Nacional de Investigaciones Científicas y Técnicas (CONICET), and by grants from DNA-IAA (PICTA 7/2008-2011), ANP-CyT-DNA (PICTO 0116/2012-2015), PICT 2017-2691, Deutsche Forschungsgemeinschaft (DFG, grant Za735/1-1), PICT-2018-01379, PICT-2021-I-A-00501, and PICT-2021-GRF-TI-00536. These studies were also supported by MINCYT-BMBF Program (AL/17/06- 01DN18024) and ALEARG'18 Scholarship by DAAD/Ministerio de Educación de Argentina. The present manuscript also presents an outcome of the EU project IMCONet (FP7 IRSES, action no. 319718). This project has received funding from the European Union's Horizon 2020 research and innovation programme under the Marie Skłodowska-Curie grant agreement No 87269 CoastCarb. We are especially grateful to the divers, scientific and logistics groups of Carlini Station – Dallmann Laboratory for their technical assistance during the Antarctic expeditions. In addition, we gratefully acknowledge Hendrik Pehlke, Fernando Momo, Micaela B. Ruiz, and Alfredo Costa for their valuable help in the result section.

Appendix A. Supplementary data

Supplementary data to this article can be found online at https://doi.org/10.1016/j.scitotenv.2024.178249.

Data availability

Data will be made available on request.

References

Amsler, C.D., Iken, K., McClintock, J.B., Amsler, M., Peters, K.J., Hubbard, J.M., et al., 2005. Comprehensive evaluation of the palatability and chemical defenses of subtidal macroalgae from the Antarctic Peninsula. Mar. Ecol. Prog. Ser. 294, 141–159. https://doi.org/10.3354/meps294141.

Ahn, I.Y, Moon, H.W., Jeon, M., Kang, S.H., 2016. First record of massive blooming of benthic diatoms and their association with megabenthic filter feeders on the shallow seafloor of an Antarctic fjord: does glacier melting fuel the bloom? Ocean Sci. J. 51, 273–279. https://doi.org/10.1007/s12601-016-0023-y.

Amsler, C.D., Amsler, M.O., Klein, A.G., Galloway, A.W., Iken, K., McClintock, J.B., et al., 2023. Strong correlations of sea ice cover with macroalgal cover along the Antarctic Peninsula: ramifications for present and future benthic communities. Elem. Sci. Anth. 11, 1. https://doi.org/10.1525/elementa.2023.00020.

Barnes, D.K.A., Souster, T., 2011. Reduced survival of Antarctic benthos linked to climate-induced iceberg scouring. Nat. Clim. Chang. 1, 365–368. https://doi.org/10.1371/journal.pone.0058223, 10.1038/nclimate1232. 2013; 8(3): e58223.

Barnes, D.K.A., Fenton, M., Cordingley, A., 2014. Climate-linked iceberg activity massively reduces spatial competition in Antarctic shallow waters. Curr. Biol. 24 (12), R553–R554. https://doi.org/10.1016/j.cub.2014.04.040.

Barnes, D.K.A., Sands, C.J., Cook, A., Howard, F., Roman, A., Carlos, G., et al., 2020. Blue carbon gains from glacial retreat along Antarctic fjords: what should we expect. Glob. Chang. Biol. 2750–2755. https://doi.org/10.1111/gcb.15055.

Barnes, D.K.A., Sands, C.J., Paulsen, M.L., Moreno, B., Held, C., Downey, R., et al., 2021. Societal importance of Antarctic negative feedbacks on climate change: blue carbon gains from sea ice, ice shelf and glacier losses. Sci. Nat. 108, 43. https://doi.org/10.1007/s00114-021-01748-8.

Barnes, D.K.A., Morley, S.A., Mathews, R., Clement, A., Peck, L.S., 2024. Trajectory of increased iceberg kill-off in West Antarctica's shallows. Curr. Biol. 10, 488–490. ISSN 0960-9822. https://doi.org/10.1016/j.cub.2024.03.036.

Bartsch, I., Paar, M., Fredriksen, S., Schwanitz, M., Daniel, C., Hop, H., et al., 2016. Changes in kelp forest biomass and depth distribution in Kongsfjorden, Svalbard, between 1996–1998 and 2012–2014 reflect Arctic warming. Polar Biol. 39, 2021–2036. https://doi.org/10.1007/s00300-015-1870-1.

Bax, N., Sands, C.J., Gogarty, B., Downey, R.V., Moreau, C.V., Moreno, B., et al., 2021. Perspective: increasing blue carbon around Antarctica is an ecosystem service of considerable societal and economic value worth protecting. Glob. Chang. Biol. 27, 5–12. https://doi.org/10.1111/gcb.15392.

Bennett, J.R., Shaw, J.D., Treads, A., Smol, J.P., Aerts, R., Bergstrom, D.M., et al., 2015. Polar lessons learned: informing long-term management based on shared threats in Arctic and Antarctic environments. Front. Ecol. Environ. 15, 316–324. https://doi.org/10.1890/140315.

Braeckman, U., Pasotti, F., Hoffmann, R., Vazquez, S., Wulff, A., Schloss, I.R., et al., 2021. Glacial melt disturbance shifts community metabolism of an Antarctic seafloor ecosystem from net autotrophy to heterotrophy. Comm. Biol. 4, 148. https://doi.org/10.1038/s42003-021-01673-6.

Campana, G.L., Zacher, K., Deregibus, D., Momo, F., Wiencke, C., Quartino, M.L., 2018. Succession of Antarctic benthic algae (Potter Cove, South Shetland Islands): structural patterns and glacial impact over a four-year period. Polar Biol. 41 (2), 377–396. https://doi.org/10.1007/s00300-017-2197-x.

Campana, G.L., Zacher, K., Momo, F.R., Deregibus, D., Debandi, J.I., Ferreyra, G.A., et al., 2020. Successional processes in Antarctic benthic algae. In: Gómez, I., Huovinen, P. (Eds.), Antarctic Seaweeds. Springer, Cham. https://doi.org/10.1007/978-3-030-39448-6_9.

Carrasco, J.F., Bozkurt, D., Cordero, R.R., 2021. A review of the observed air temperature in the Antarctic peninsula. In: Did the Warming Trend Come Back after the Early 21st hiatus? Sci, Polar. https://doi.org/10.1016/j.polar.2021.100653.

CCAMLR-43/37. n.d. Revised proposal for a Conservation Measure establishing a Marine Protected Area in Domain 1 (Western Antarctic Peninsula and South Scotia Arc). Delegations of Argentina and Chile.

Chown, S.L., Leihy, R.I., Naish, T.R., Brooks, C.M., Convey, P., Henley, B.J., et al., (Eds.). 2022. Antarctic Climate Change and the Environment: A Decadal Synopsis and Recommendations for Action. Scientific Committee on Antarctic Research, Cambridge, United Kingdom. www.scar.org.

Clark, G.F., Stark, J.S., Johnston, E.L., Runcie, J.W., Goldsworthy, P.M., Raymond, B., et al., 2013. Light-driven tipping points in polar ecosystems. Glob. Chang. Biol. 19 (12), 3749–3761. https://doi.org/10.1111/gcb.12337. 2013.

Clark, G.F., Stark, J.S., Palmer, A.S., Riddle, M.J., Johnston, E.L., 2017. The roles of sea-ice, light and sedimentation in structuring shallow Antarctic benthic communities. PLoS One 12 (1), e0168391. https://doi.org/10.1371/journal.pone.0168391.

Constable, A.J., Melbourne-Thomas, J., Corney, S.P., Arrigo, K.R., Barbraud, C., Barnes, D.K., et al., 2014. Climate change and Southern Ocean ecosystems. I: how changes in physical habitats directly affect marine biota. Glob. Chang. Biol. 20, 3004–3025. https://doi.org/10.1111/gcb.12623.

Constable, A.J., Melbourne-Thomas, J., Muelbert, M.M.C., McCormack, S., Brasier, M., Caccavo, J.A., et al., 2023. Marine Ecosystem Assessment for the Southern Ocean: Summary for Policymakers. Integrated Climate and Ecosystem Dynamics in the Southern Ocean, Scientific Committee on Antarctic Research, Scientific Committee on Oceanic Research, Integrated Marine Biosphere Research. https://doi.org/10.5281/zenodo.8359585.

Convey, P., Peck, L.S., 2019. Antarctic environmental change and biological responses. Sci. Adv. 5 (11). https://doi.org/10.1126/sciadv.aaz0888 eaaz0888-eaaz0888.

Cook, A.J., Holland, P.R., Meredith, M.P., Murray, T., Luckman, A., Vaughan, D.G., 2016. Ocean forcing of glacier retreat in the western Antarctic Peninsula. Science 353 (6296), 283–286. https://doi.org/10.1126/science.aae0017.

Costa, A., Agosta, E., 2012. South pacific quasi-stationary waves and anomalously cold summers in the northernmost Antarctic peninsula. Geoacta 37 (2), 73–82.

Deregibus, Dolores, 2017. Efecto del retroceso glaciario inducido por el cambio climático sobre la comunidad de macroalgas en nuevas áreas libres de hielo en un ecosistema costero antártico (Caleta Potter, I. 25 de Mayo, I. Shetland del Sur). Universidad de Buenos Aires. Facultad de Ciencias Exactas y Naturales. Tesis Doctoral.

Deregibus, D., Quartino, M.L., Campana, G.L., Momo, F.R., Wiencke, C., Zacher, K., 2016. Photosynthetic light requirements and vertical distribution of macroalgae in newly ice-free areas in Potter Cove, South Shetland Islands, Antarctica. Polar Biol. 39 (1), 153–166. https://doi.org/10.1007/s00300-015-1679-y.

Deregibus, D., Quartino, M.L., Zacher, K., Campana, G.L., Barnes, D.K.A., 2017. Understanding the link between sea ice, ice scour and Antarctic benthic biodiversity; the need for cross station and nation collaboration. Polar Rec. 53, 143–152. https://doi.org/10.1017/S0032247416000875.

Deregibus, D., Zacher, K., Bartsch, I., Campana, G.L., Momo, F.R., Wiencke, C., et al., 2020. Carbon balance under a changing light environment. In: Gómez, I., Huovinen, P. (Eds.), Antarctic Seaweeds. Springer, Cham. https://doi.org/10.1007/978-3-030-39448-6_9.

Deregibus, D., Campana, G.L., Neder, C., Barnes, D.K., Zacher, K., Piscicelli, J.M., et al., 2023. Potential macroalgal expansion and blue carbon gains with northern Antarctic Peninsula glacial retreat. Mar. Environ. Res. 106056. https://doi.org/10.1016/j.marenvres.2023.106056.

Di Rienzo, J.A., Casanoves, F., Balzarini, M.G., Gonzalez, L., Tablada, M.R., Robledo, C. W., 2008. InfoStat versión 2008. Grupo InfoStat, Facultad de Ciencias Agropecuarias, Universidad Nacional de Córdoba, Córdoba.

Drew, E.A., Hastings, R.M., 1992. A year-round ecophysiological study of Himantothallus grandifolius (Desmarestiales, Phaeophyta) at Signy Island, Antarctica. Phycologia 31, 262.

Duarte, C.M., Gattuso, J.P., Hancke, K., Gundersen, H., Filbee-Dexter, K., Pedersen, M.F., et al., 2022. Global estimates of the extent and production of macroalgal forests. Glob. Ecol. Biogeogr. 31, 1422–1439. https://doi.org/10.1111/geb.13515.
Ducklow, H.W., Fraser, W.R., Meredith, M.P., Stammerjohn, S.E., Doney, S.C., Martinson, D.G., et al., 2013. West Antarctic Peninsula: an ice-dependent coastal marine ecosystem in transition. Oceanography 26 (3), 190–203. https://doi.org/10.5670/oceanog.2013.62.
Düsedau, L., Fredriksen, S., Brand, M., Fischer, P., Karsten, U., Bischof, K., et al., 2024. Kelp forest community structure and demography in Kongsfjorden (Svalbard) across 25 years of Arctic warming. Ecol. Evol. 14 (6). https://doi.org/10.1002/ece3.11606.
Franke, K., Bartsch, I., Karsten, U., Graiff, A., 2024. Seasonality influences the effect of warming on kelp photosynthesis. Mar. Ecol. Prog. Ser. 739, 15–29. https://doi.org/10.3354/meps14623.
Gómez Izquierdo, D. R., Quartino, M. L., Abele, D. Photographs of Potter Cove, King George Island, Looking West Towards Maxwell Bay in 2009–2019 (Instituto Antártico Argentino, Buenos Aires, Argentina).
Gómez, I., Huovinen, P., 2020. Antarctic seaweeds: biogeography, adaptation, and ecosystem services. In: Gómez, I., Huovinen, P. (Eds.), Antarctic Seaweeds. Springer, Cham. https://doi.org/10.1007/978-3-030-39448-6_1.
Gómez, I., Weykam, G., Kloser, H., Wiencke, C., 1997. Photosynthetic light requirements, metabolic carbon balance and zonation of sublittoral macroalgae from King George Island (Antarctica). Mar. Ecol. Prog. Ser. 148, 281–293. https://doi.org/10.3354/meps148281.
Gómez, I., Wulff, A., Roleda, M.Y., Huovinen, P., Karsten, U., Quartino, M.L., et al., 2009. Light and temperature demands of marine benthic microalgae and seaweeds in polar regions. Bot. Ma. 52, 593–608. https://doi.org/10.1515/BOT.2009.073.
Griffiths, H.J., Cummings, V.J., Van de Putte, A., Whittle, R.J., Waller, C.L., 2024. Antarctic benthic ecological change. Nat. Rev. Earth Environ. 5, 645–664. https://doi.org/10.1038/s43017-024-00583-5.
Hanley, M.E., Firth, L.B., Foggo, A., 2023. Victim of changes? Marine macroalgae in a changing world. Ann. Bot. 133 (1), 1–16. https://doi.org/10.1093/aob/mcad185.
Hass, H.C., Kuhn, G., Monien, P., Brumsack, H.J., Forwick, M., 2010. Climate fluctuations during the past two millennia as recorded in sediments from Maxwell Bay, South Shetland Islands, West Antarctica. In: Geo. Soc. of London, London: Special Publication, No. 344. https://doi.org/10.1144/SP344.17.
Hendry, K.R., Meredith, M.P., Ducklow, H.W., 2018. The marine system of the West Antarctic Peninsula: status and strategy for progress. Philos. Trans. R. Soc. A Math. Phys. Eng. Sci. 376, 1–6. https://doi.org/10.1098/rsta.2017.0179.
Huovinen, P., Gómez, I., 2020. Underwater Light Environment of Antarctic Seaweeds. Springer, Cham. https://doi.org/10.1007/978-3-030-39448-6.
IPCC, 2021a. Regional fact sheet—polar regions. In: Masson Delmotte, V., Zhai, P., Pirani, A., et al. (Eds.), Climate Change 2021: The Physical Science Basis. Contribution of Working Group I to the Sixth Assessment Report of the Intergovernmental Panel on Climate Change.
IPCC, 2021b. In: Masson-Delmotte, V., et al. (Eds.), Climate Change 2021: The Physical Science Basis. Contribution of Working Group I to the Sixth Assessment Report of the Intergovernmental Panel on Climate Change. IPCC, Geneva.
IPCC WGI Interactive Atlas n.d.: Regional Information (Advanced).
Jassby, A.D., Platt, T., 1976. Mathematical formulation of the relationship photosynthesis and light for phytoplankton. Limnol. Oceanogr. 21, 540–547. https://doi.org/10.4319/lo.1976.21.4.0540.
Jerosch, K., Scharf, F.K., Deregibus, D., Campana, G.L., Zacher, K., Pehlke, et al., 2019. Ensemble modeling of Antarctic macroalgal habitats exposed to glacial melt in a polar fjord. Front. Ecol. Evol. 7, 207. https://doi.org/10.3389/fevo.2019.00207.
Kirk, J.T.O., 1994. Light and Photosynthesis in Aquatic Ecosystems. Cambridge University Press, Cambridge. https://doi.org/10.1017/CBO9780511623370.
Klöser, H., Ferreyra, G., Schloss, I., Mercuri, G., Laturns, F., Curtosi, A., 1993. Seasonal variation of algal growth conditions in sheltered Antarctic bays: the example of Potter Cove King George Island, South Shetlands. J. Mar. Syst. 4. https://doi.org/10.1016/0924-7963(93)90025-H.
Klöser, H., Quartino, M.L., Wiencke, C., 1996. Distribution of macroalgae and macroalgal communities in gradients of physical conditions in Potter Cove, King George Island, Antarctica. Hydrobiologia 333, 1–17. https://doi.org/10.1007/BF00020959.
Konik, M., Darecki, M., Pavlov, A.K., Sagan, S., Kowalczuk, P., 2021. Darkening of the Svalbard fjords waters observed with satellite ocean color imagery in 1997–2019. Front. Mar. Sci. 8, 699318. https://doi.org/10.3389/fmars.2021.699318.
Krause-Jensen, D., Duarte, C.M., 2016. Substantial role of macroalgae in marine carbon sequestration. Nat. Geosci. 9 (10), 737. https://doi.org/10.1038/ngeo2790.
Lagger, C., Servetto, N., Torre, L., Sahade, R., 2017. Benthic colonization in newly ice-free soft-bottom areas in an Antarctic fjord. PLoS One 12, e0186756. https://doi.org/10.1371/journal.pone.0186756.
Lagger, C., Nime, M., Torre, L., Servetto, N., Tatián, M., Sahade, R., 2018. Climate change, glacier retreat and a new ice-free island offer new insights on Antarctic benthic responses. Ecography 40, 1–12. https://doi.org/10.1111/ecog.03018.
Lee, S.H., Joo, H.M., Joo, H., Kim, B.K., Song, H.J., Jeon, M., et al., 2015. Large contribution of small phytoplankton at Marian Cove, King George Island, Antarctica, based on long-term monitoring from 1996 to 2008. Polar Biol. 38, 207–220. https://doi.org/10.1007/s00300-014-1579-6.
Lima, D.T., Moser, G.A.O., Piedras, F.R., Cunha, L.C.D., Tenenbaum, D.R., Tenório, M.M. B., et al., 2019. Abiotic changes driving microphytoplankton functional diversity in Admiralty Bay, King George Island (Antarctica). Front. Mar. Sci. 6, 638. https://doi.org/10.3389/fmars.2019.00638.
Long, M.H., Rheuban, J.E., Berg, P., Zieman, J.C., 2012. A comparison and correction of light intensity loggers to photosynthetically active radiation sensors. Limnol. Oceanogr. Methods 10 (6), 416–424. https://doi.org/10.4319/lom.2012.10.416.
Marina, T.I., Salinas, V., Cordone, G., Campana, G.L., Moreira, E., Deregibus, D., et al., 2018. The food web of Potter cove (Antarctica): complexity, structure and function. Estuar. Coast. Shelf Sci. 200, 141–151. https://doi.org/10.1016/j.ecss.2017.10.015.
Marshall, G.J., 2003. Trends in the Southern Annular Mode from observations and reanalyses. J. Clim. 16, 4134–4143. https://doi.org/10.1175/1520-0442(2003)016<4134:TITSAM>2.0.CO;2.
Marshall, G.J., Orr, A., van Lipzig, N.P.M., King, J.C., 2006. The impact of a changing southern hemisphere annular mode on Antarctic peninsula summer temperatures. J. Clim. 19, 5388–5404. https://doi.org/10.1175/JCLI3844.1.
Maturilli, M., Herber, A., König-Langlo, G., 2015. Surface radiation climatology for Ny-Ålesund, Svalbard (78.9° N), basic observations for trend detection. Theor. Appl. Climatol. 120, 331–339. https://doi.org/10.1007/s00704-014-1173-4.
Meredith, M.P., Falk, U., Bers, A.V., Mackensen, A., Schloss, I.R., Barlett, E.R., et al., 2018. Anatomy of a glacial meltwater discharge event in an Antarctic cove. Philos. Trans. R. Soc. A Math. Phys. Eng. Sci. 376. https://doi.org/10.1098/rsta.2017.0163.
Morley, S.A., Souster, T.A., Vause, B.J., Gerrish, L., Peck, L.S., Barnes, D.K.A., 2022. Benthic biodiversity, carbon storage and the potential for increasing negative feedbacks on climate change in shallow waters of the Antarctic Peninsula. Biology 11, 320. https://www.mdpi.com/2079-7737/11/2/320.
Muscatine, L., 1980. Productivity of zooxanthellae. In: Falkowski, P.G. (Ed.), Primary Productivity in the Sea. Plenum Press, New York, pp. 403–410. https://doi.org/10.1007/978-1-4899-0762-2_14.
Neder, C., Sahade, R., Abele, D., Pesch, R., Jerosch, K., 2020. Default versus configured -geostatistical modeling of suspended particulate matter in potter cove, West Antarctic Peninsula. Fluids 5 (4), 235. https://doi.org/10.3390/fluids5040235.
Neder, C., et al., 2022. Modelling suspended particulate matter dynamics at an Antarctic fjord impacted by glacier melt. J. Ma. Syst. https://doi.org/10.1016/j.jmarsys.2022.103734.
Neder, C., Jerosch, K., Pehlke, H., Torre, L., Sahade, R., 2024. Antarctic benthic species distribution models and compositional analysis in a coastal ecosystem under glacier retreat. Mar. Ecol. Prog. Ser. 750, 1–18. https://doi.org/10.3354/meps14731.
Niedzwiedz, S., Bischof, K., 2023. Glacial retreat and rising temperatures are limiting the expansion of temperate kelp species in the future Arctic. Limnol. Oceanogr. 68, 1–15. https://doi.org/10.1002/lno.12312.
NSIDC, 2023. National Snow and Ice Data Center. University of Colorado Boulder.
Pavlov, A.K., Leu, E., Hanelt, D., Bartsch, I., Karsten, U., Hudson, S.R., et al., 2019. The underwater light climate in Kongsfjorden and its ecological implications. In: Hop, H., Wiencke, C. (Eds.), The Ecosystem of Kongsfjorden, Svalbard. Advances in Polar Ecology, vol 2. Springer, Cham. https://doi.org/10.1007/978-3-319-46425-1_5.
Parkinson, C.L., DiGirolamo, N.E., 2021. Sea ice extents continue to set new records: Arctic, Antarctic, and global results. Remote Sens. Environ. 267, 112753. https://doi.org/10.1016/j.rse.2021.112753.
Pellizzari, F., De Mello, J.P.D.S., Santos-Silva, M.C., Osaki, V.S., Brandini, F.P., Convey, P., et al., 2023. New records and updated distributional patterns of macroalgae from the South Shetland Islands and northern Weddell Sea, Antarctica. Antarct. Sci. 35 (4), 243–255. https://doi.org/10.1017/S095410202300010X.
Pessarrodona, A., Filbee-Dexter, K., Krumhansl, K.A., Pedersen, M.F., Moore, P.J., Wernberg, T., 2022. l. A global dataset of seaweed net primary productivity. Sci Data 9 (1), 484. https://doi.org/10.1038/s41597-022-01554-5.
Piñones, A., Aziares-Aguayo, N., Amador-Véliz, P., Mercado-Peña, O., González-Reyes, A., Valdivia, N., et al., 2024. Local and remote atmosphere-ocean couplingduring extreme warming events impacting subsurface ocean temperature in anAntarctic embayment. J. Geophysical Research: Oceans 129. https://doi.org/10.1029/2023jc020735 e2023JC020735.
Quartino, M.L., Deregibus, D., Campana, G.L., Latorre, G.E.J., Momo, F.R., 2013. Evidence of macroalgal colonization on newly ice-free areas following glacial retreat in Potter Cove (South Shetland Islands), Antarctica. PLoS One. https://doi.org/10.1371/journal.pone.0058223.
Quartino, M.L., Saravia, L.A., Campana, G.L., Deregibus, D., Matula, C.V., et al., 2020. Production and biomass of seaweeds in newly ice-free areas: implications for coastal processes in a changing Antarctic environment. In: Gómez, I., Huovinen, P. (Eds.), Antarctic Seaweeds. Springer, Cham. https://doi.org/10.1007/978-3-030-39448-6_8.
Rodrigo, C., Giglio, S., Varas, A., 2016. Glacier sediment plumes in small bays on the Danco Coast, Antarctic Peninsula. Antarct. Sci. 28 (5), 395–404. https://doi.org/10.1017/S0954102016000237.
Roese, M., Drabble, M., 1998. Wind driven circulation in potter cove. In: Wiencke, C., Ferreyra, G., Arntz, W., Rinaldi, C. (Eds.), The Potter Cove Coastal Ecosystem, Antarctica. Alfred-Wegener Institut (AWI), Bremerhaven, pp. 40–46.
Ross, F.W., Boyd, P.W., Filbee-Dexter, K., Watanabe, K., Ortega, A., Krause-Jensen, D., et al., 2023. Potential role of seaweeds in climate change mitigation. Sci. Total Environ. 885, 163699. https://doi.org/10.1016/j.scitotenv.2023.163699.
Rückamp, M., Braun, M., Suckro, S., Blindow, N., 2011. Observed glacial changes on the King George Island ice cap, Antarctica, in the last decade. Glob. Planet. Chang. 79. https://doi.org/10.1016/j.gloplacha.2011.06.009.
Ruiz Barlett, E.M., Tosonotto, G.V., Piola, A.R., Sierra, M.E., Mata, M.R., 2018. On the temporal variability of intermediate and deep waters in the Western Basin of the Bransfield Strait. Deep-Sea Res. II 149, 31–46. https://doi.org/10.1016/j.dsr2.2017.12.010.
Ruiz Barlett, E.M., Sierra, M.E., Costa, A.J., Tosonotto, G.V., 2021. Interannual variability of hydrographic properties in Potter Cove during summers between 2010 and 2017. Antarct. Sci. 1–20. https://doi.org/10.1017/S0954102020000668.
Runcie, J.W., Riddle, M.J., 2006. Photosynthesis of marine macroalgae in ice-covered and ice-free environments in East Antarctica. Eur. J. Phycol. 41 (223), 233. https://doi.org/10.1080/09670260600645824.

Runcie, J.W., Riddle, M.J., 2012. Estimating primary productivity of marine macroalgae in East Antarctica using in situ fluorometry. Eur. J. Phycol. 47 (4), 449–460.

Sahade, R., Lagger, C., Torre, L., Momo, F., Monien, P., Schloss, I., et al., 2015. Climate change and glacier retreat drive shifts in an Antarctic benthic ecosystem. Sci. Adv. 1, e1500050. https://doi.org/10.1126/sciadv.1500050.

Sands, C.J., Zwerschke, N., Bax, N., Barnes, D.K.A., Moreau, C., Downey, R., et al., 2023. Perspective: the growing potential of Antarctic blue carbon. In: Kappel, E.S., Cullen, V., Costello, M.J., Galgani, L., Gordó-Vilaseca, C., Govindarajan, A., Kouhi, S., Lavin, C., McCartin, L., Müller, J.D., Pirenne, B., Tanhua, T., Zhao, Q., Zhao, S. (Eds.), Frontiers in Ocean Observing: Emerging Technologies for Understanding and Managing a Changing Ocean, Oceanography, 36 (Supplement 1), pp. 16–17. https://doi.org/10.5670/oceanog.2023.s1.5.

SC-CAMLR-42/BG/11 n.d. Antarctic Climate Change and the Environment: Update on Recent Research Relevant to CCAMLR. SCAR.

Scherrer, K., 2015. Light, Temperature and Competition – Understanding the Causes for Climate-driven Regime Shifts in Arctic Marine Benthos. Uppsala University. UPTEC W 15 048. ISSN 1401-5765.

Schlegel, R.W., Singh, R.K., Gentili, B., Bélanger, S., Castro de la Guardia, L., Krause-Jensen, D., et al., 2024. Underwater light environment in Arctic fjords. Earth Syst. Sci. Data 16, 2773–2788. https://doi.org/10.5194/essd-16-2773-2024.

Schloss, I.R., Abele, D., Moreau, S., Demers, S., Bers, A.V., González, O., et al., 2012. Response of phytoplankton dynamics to 19-year (1991–2009) climate trends in Potter Cove (Antarctica). J. Mar. Syst. 92, 53–66. https://doi.org/10.1016/j.jmarsys.2011.10.006.

Siegert, M.J., Bentley, M.J., Atkinson, A., Bracegirdle, T.J., Convey, P., Davies, et al., 2023. Antarctic extreme events. Front. Environ. Sci. 11, 1229283. https://doi.org/10.3389/fenvs.2023.1229283.

Smith, C.A., Sardeshmukh, P., 2000. The effect of ENSO on the intraseasonal variance of surface temperature in winter. Int. J. Climatol. 20. https://doi.org/10.1002/1097-0088(20001115) 20:13<1543: AID-JOC579>3.0.CO;2-A.

Stammerjohn, S.E., Martinson, D.G., Smith, R.C., Yuan, X., Rind, D., 2008. Trends in Antarctic annual sea ice retreat and advance and their relation to El Niño–Southern Oscillation and Southern Annular Mode variability. J. Geophys. Res. 113. https://doi.org/10.1029/2007JC004269.

Stammerjohn, S., Massom, R., Rind, D., Martinson, D., 2012. Regions of rapid sea ice change: an inter-hemispheric seasonal comparison. Geophys. Res. Lett. 39. https://doi.org/10.1029/2012GL050874.

Swadling, K.M., Constable, A.J., Fraser, A.D., Massom, R.A., Borup, M.D., Ghigliotti, L., et al., 2023. Biological responses to change in Antarctic Sea ice habitats. Front. Ecol. Evol. 10. https://doi.org/10.3389/fevo.2022.1073823.

Tait, L.W., Chin, C., Nelson, W., George, S., Marriott, P., O'Driscoll, R.L., et al., 2024. Deep-living and diverse Antarctic seaweeds as potentially important contributors to global carbon fixation. Commun. Earth Environ. 5, 205. https://doi.org/10.1038/s43247-024-01362-2.

Tejedo, P., Benayas, J., Cajiao, D., Leung, Y.F., De Filippo, D., Liggett, D., 2022. What are the real environmental impacts of Antarctic tourism? Unveiling their importance through a comprehensive meta-analysis. J. Environ. Manag. 308, 114634. https://doi.org/10.1016/j.jenvman.2022.114634.

Thompson, T., 2022. Antarctic Sea ice hits lowest minimum on record. Nature. PMID: 35277689. https://www.nature.com/articles/d41586-022-00550-4.

Turner, J., Bindschadler, R.A., Convey, P., Di Prisco, G., Fahrbach, E., Gutt, J., et al., 2009. Antarctic Climate Change and the Environment. SCAR, Cambridge.

Turner, J., Lu, H., White, I., et al., 2016. Absence of 21st century warming on Antarctic Peninsula consistent with natural variability. Nature 535, 411–415. https://doi.org/10.1038/nature18645.

Turner, J., Phillips, T., Marshall, G.J., Hosking, J.S., Pope, J.O., Bracegirdle, T.J., et al., 2017. Unprecedented springtime retreat of Antarctic Sea ice in 2016. Geophys. Res. Lett. https://doi.org/10.1002/2017GL073656.

Vaughan, D., Marshall, G.J., Connolley, W.M., Parkinson, C., Mulvaney, R., Hodgson, D. A., et al., 2003. Recent rapid regional climate warming on the Antarctic Peninsula. Clim. Chang. 60 (3), 243–274. https://doi.org/10.1023/A:1026021217991.

Wiencke, C., Amsler, C.D., 2012. Seaweeds and their communities in polar regions. In: Wiencke, C., Bischof, K. (Eds.), Seaweed Biology, Novel Insights into Ecophysiology, Ecology and Utilization Ecological Studies 219. Springer, Heidelberg, pp. 265–292. https://doi.org/10.1007/978-3-642-28451-9.

Wójcik, K.A., Bialik, R.J., Osińka, M., Figielski, M., 2019. Investigation of sediment-rich glacial meltwater plumes using a high-resolution multispectral sensor mounted on an unmanned aerial vehicle. Water 11, 2405. https://doi.org/10.3390/w11112405.

Wölfl, A.C., Lim, C.H., Hass, H.C., Lindhorst, S., Tosonotto, G., Littman, K.A., et al., 2014. Distribution and characteristics of marine habitats in a subpolar bay based on hydroacoustics and bed shear stress estimates - Potter Cove, King George Island, Antarctica. Geo-Mar. Lett. 34 (5), 435–446. https://doi.org/10.1007/s00367-014-0375-1.

Worm, B., Barbier, E.B., Beaumont, N., Duffy, J.E., Folke, C., Halpern, B.S., et al., 2006. Impacts of biodiversity loss on ocean ecosystem services. Science 314, 787–790. https://doi.org/10.1126/science.1132294.

Yu, L., Zhong, S., Sui, C., 2024. Surface air temperature anomalies over Antarctica and the Southern Ocean induced by interactions between the interdecadal Pacific oscillation and Atlantic multidecadal oscillation. Geosci. Lett. 11, 39. https://doi.org/10.1186/s40562-024-00352-8.

Yuan, X., 2004. ENSO-related impacts on Antarctic Sea ice: a synthesis of phenomenon and mechanisms. Antarct. Sci. 16, 415–425. https://doi.org/10.1017/S0954102004002238.

Zacher, K., Rautenberger, R., Hanelt, D., Wulff, A., Wiencke, C., 2009. The abiotic environment of polar marine benthic algae. Bot. Mar. 52, 483–490. https://doi.org/10.1515/BOT.2009.082.